# Eastern tropical Pacific hydrologic changes during the past 27,000 years from D/H ratios in alkenones

Katharina Pahnke[1§*], Julian Sachs[1†], Lloyd Keigwin[2],
Axel Timmermann[3], Shang-Ping Xie[3]

[1]Department of Earth, Atmospheric and Planetary Sciences, Massachusetts Institute of Technology, Cambridge, MA 02139, USA
[2]Woods Hole Oceanographic Institution, Woods Hole, MA 02543, USA
[3]International Pacific Research Center, SOEST, University of Hawai`i at Manoa, Honolulu, HI 96822, USA

[§] now at: Lamont-Doherty Earth Observatory of Columbia University, Palisades, NY 10964, USA
[†] now at: School of Oceanography, University of Washington, Seattle, WA 98195, USA

submitted to *Paleoceanography* April 11, 2007

*contact: kpahnke@ldeo.columbia.edu, jsachs@u.washington.edu

**Abstract**

The tropical Pacific plays a central role in the climate system by providing large diabatic heating that drives the global atmospheric circulation. Quantifying the role of the tropics in late Pleistocene climate change has been hampered by the paucity of paleoclimate records from this region and the lack of realistic transient climate model simulations covering this period. Here we present records of hydrogen isotope ratios (δD) of alkenones from the Panama Basin off the Colombian coast that document hydrologic changes in equatorial South America and the eastern tropical Pacific over the past 27,000 years, and the past three centuries in detail. Comparison of alkenone δD values with instrumental records of precipitation over the past ~100 years suggests that δD can be used as a hydrologic proxy. On long time scales, our records indicate reduced rainfall during the last glacial period that can be explained by a southward shift of the mean position of the Intertropical Convergence Zone and an associated reduction of Pacific moisture transport into Colombia. Precipitation increases at ~17 ka in concert with sea surface temperature (SST) cooling in the North Atlantic and the eastern tropical Pacific. A regional coupled model, forced by negative SST anomalies in the Caribbean, simulates an intensification of northeasterly trade winds across Central America, increased evaporative cooling, and a band of increased rainfall in the northeastern tropical Pacific. These results are consistent with the alkenone SST and δD reconstructions that suggest increasing precipitation and SST cooling at the time of Heinrich event 1.

## 1 Introduction

An ever increasing number of low-latitude paleoclimate records demonstrates that tropical climate underwent substantial temperature and precipitation changes on glacial-interglacial and millennial time scales [e.g., *Benway et al.*, 2006; *Haug et al.*, 2001; *Leduc et al.*, 2007; *Peterson et al.*, 2000; *Peterson and Haug*, 2006; *Wang et al.*, 2004]. Sea surface temperatures (SST) in the tropics were 2°-3°C colder during the last glacial maximum (LGM) than during the Holocene [*Koutavas et al.*, 2002; *Stott et al.*, 2002], while terrestrial records indicate air temperature changes of 5-6°C [*Colinvaux et al.*, 1996; *Stute et al.*, 1995]. Precipitation was reduced and northeasterly winds stronger in the Northern Hemisphere tropics during the last glacial and short-lived ($10^2$-$10^3$ yr) cold episodes in the North Atlantic such as the Younger Dryas and Heinrich meltwater events (H-events) [*Bush et al.*, 1992; *Haug et al.*, 2001; *Hooghiemstra and van der Hammen*, 1993; *Hughen et al.*, 1996; *Mora and Pratt*, 2001; *Peterson et al.*, 2000]. At the same time, the southern tropics experienced wetter conditions [*Maslin and Burns*, 2000; *Mayle et al.*, 2004; *Wang et al.*, 2006; *Wang et al.*, 2004]. This precipitation pattern is consistent with meridional shifts of the Intertropical Convergence Zone (ITCZ).

Climate modeling evidence [e.g., *Stouffer et al.*, 2007; *Timmermann et al.*, 2005; *Timmermann et al.*, 2007b; *Zhang and Delworth*, 2005] supports the notion that meltwater pulses in the northern North Atlantic can disrupt the large-scale Atlantic meridional overturning circulation (AMOC) reducing surface density and deep-water formation. A weaker AMOC leads to a decrease of the poleward heat-transport in the North Atlantic [*Stocker and Johnsen*, 2003] and a cooling of surface waters. This cooling enhances the trade wind circulation [*Chiang and Bitz*, 2005; *Krebs and Timmermann*, 2007] and increases evaporation, thereby spreading the cooling southward. The enhanced northeasterly trades and SST cooling in the tropical North Atlantic lead to southward displacement of the Intertropical Convergence Zone, documented by instrumental observations [*Chiang*, 2005; *Xie and Carton*, 2004], and reflected in tropical paleo-proxy records by precipitation changes. The southward shift of the ITCZ in the Atlantic has also been shown to play a key role in the recovery of the AMOC after a major shutdown [*Krebs and Timmermann*, 2007].

Cooling in the Caribbean generates an anticyclonic surface circulation in the atmosphere, which spreads into the tropical North Pacific across Central America [*Timmermann et al.*, 2005; *Timmermann et al.*, 2007b; *Zhang and Delworth*, 2005]. Over the tropical Pacific, enhanced northeasterly trade winds lead to enhanced Ekman pumping north of the equator, evaporative cooling, and a southward shift of the ITCZ. Due to positive air-sea coupling, the meridionally asymmetric SST, wind, and precipitation patterns can propagate into the western Pacific, thereby affecting salinity and rainfall in the Warm Pool [*Stott et al.*, 2004] and Australia [*Turney et al.*, 2004].

On orbital timescales, two other important processes further contribute to the meridional position of the ITCZ. Orographic forcing of the glacial ice-sheets over North America enhances the upper-level stationary eddy momentum flux convergence at about 30°N, which leads to descending motion near 30°N and ascending motion around the equator. The resulting pressure gradient intensifies the northern trade wind circulation, which results in an enhancement of the oceanic subtropical cells, increased upwelling and colder sea surface conditions in the tropical and North Pacific [*Timmermann et al.*, 2004].

Furthermore, the seasonal cycle of clouds generates a meridional asymmetry of net-annual mean shortwave radiation on precessional timescales [*Timmermann et al.*, 2007a]. The resulting heating asymmetry also affects the meridional position of the ITCZ considerably.

While many paleo-proxy and modeling studies have helped to elucidate the response of the Atlantic Ocean to orbital and millennial-scale forcing, the dynamics of the tropical Pacific on these time scales still remain elusive. While *Koutavas et al*. [2002] find a weak relative warming around Galapagos during Heinrich event 1, *Kienast et al.* [2006] reconstruct a cooling of ~3°C at their northern tropical Pacific site. Many paleo-records from the northern tropics indicate drier conditions during the last glacial period compared to the Holocene [e.g., *Haug et al.*, 2001; *Peterson et al.*, 2000]. However, two recent paleo-salinity records show no change in salinity between the LGM and Holocene [*Benway et al.*, 2006; *Leduc et al.*, 2007]. These seemingly conflicting results suggest that the patterns of orbital and millennial-scale climate change in the tropical Pacific need to be determined with more accuracy by using high-resolution proxy data as well as climate model simulations.

To help synthesize the existing paleo-proxy evidence for large-scale climate changes in the tropical Pacific during Termination 1, we present records of alkenone-SST and hydrogen isotope ratios in alkenones from the eastern tropical Pacific (5°N) for the past 27,000 years, and regional coupled modeling experiments that simulate the tropical Pacific response to an idealized cooling in the Caribbean, mimicking a Heinrich event.

The paleo-data document hydrologic changes in the Panama Basin and Colombia and provide evidence for cooling and increased rainfall during the last glacial-interglacial termination at ~17-13.5 ka, the time of Heinrich-event 1 (H1).

## 2 Oceanography and Hydroclimatology of the Panama Basin

Equatorial South America and the eastern tropical Pacific experience large precipitation changes in connection with the meridional migration of the ITCZ [*Xie et al.*, 2005], making the eastern tropical Pacific an ideal area to study linkages between low-latitude hydrologic changes and large-scale climate variations. In Panama and western Colombia, the seasonal precipitation pattern shows lowest rainfall in January to March and two maxima in May to June, and October to November. The rainfall maxima are interrupted by a short reduction during August and September (Figure 1). This pattern is the expression of the combined effects of the seasonal migration of the ITCZ and seasonal low-level wind jets that transport Pacific and Atlantic moisture into tropical South America [*Small et al.*, 2007 in press]. Large rivers that drain the western flanks of the Colombian Andes transfer this precipitation signal to the Panama Basin, resulting in sea surface salinities (SSS) as low as 28 psu close to the coast [*Levitus et al.*, 1994] (Figure 2). The river San Juan in Colombia [average discharge: 2,500m3/s, *Restrepo and Kjerfve*, 2002] constitutes the largest freshwater discharge to the Pacific from the Americas.

In the western Colombian Andes, a westerly low-level wind jet, the Chocó Jet, causes enormous rates of precipitation (6-13 m/year) making it one of the wettest places on earth [*Poveda and Mesa*, 2000]. The Chocó Jet is part of the southeasterly trade winds that cross the equator when the ITCZ is located in the Northern Hemisphere. Due to the Coriolis force, the winds become westerly and enter Colombia. The strength of the Chocó

Jet is positively correlated with the meridional temperature gradient between the Niño 1+2 region (east Pacific cold-tongue area) and western Colombia (including the east Pacific off Colombia) [*Poveda and Mesa*, 2000; *Vernekar et al.*, 2003]. It thus contributes to the positive (negative) rainfall anomalies in Colombia during cold (warm) ENSO phases when this temperature gradient is enhanced (reduced) [*Poveda and Mesa*, 1997; *Vernekar et al.*, 2003]. As the wind convergence of the ITCZ moves to the Southern Hemisphere where it reaches its southernmost position in February to March, the Chocó Jet ceases and precipitation in Colombia from south Pacific sources decreases substantially. Instead, the strengthened northeasterly trade winds enter the Panama Basin through a topographic gap in the Isthmus of Panama [*Chelton et al.*, 2000; *Xie et al.*, 2005]. This low-level Panama Jet forces the circulation in the Panama Basin to change from a prevailing anti-cyclonic circulation during summer to a cyclonic circulation from January to March [*Rodríguez-Rubio et al.*, 2003]. It further results in upwelling and surface cooling along a narrow strip extending from Panama southwestward [*Rodríguez-Rubio and Stuardo*, 2002]. Though precipitation in Panama and Colombia is at its annual minimum at that time (January-March), rainfall still reaches 440-480 mm/month in western Colombia (compared to annual maxima of 570-660 mm/month) *[NCEP/NCAR Reanalysis Project*] (Figure 1), demonstrating the considerable amount of moisture transported from the Atlantic across the Isthmus by the Panama Jet.

## 3 D/H as hydrologic proxy

The hydrogen isotopic ratio of water vapor (δD, expressed as deviation from Vienna Standard Mean Ocean Water, VSMOW, $\delta D = (D/H_{sample})/(D/H_{standard})-1) \times 1000$) is depleted in deuterium owing to the lower vapor pressure of DHO compared to $H_2O$ [*Gat*, 1996]. Evaporation therefore leads to a relative D-depletion of precipitation and D-enrichment of lake water and seawater.

The dominant control on δD values of precipitation in the tropics is the 'amount effect' - the inverse relationship between the isotopic ratio of precipitation and the amount of precipitation at a site [*Dansgaard*, 1964; *Rozanski et al.*, 1992]. Orographic lifting and long air mass trajectories further result in low δD values of precipitation, leading to rainfall δD values in western Colombia of -25‰ to -89‰ (long-term annual mean: -57‰) [Bogota, Colombia, *IAEA*, 2006]. Temperature-dependent fractionation, on the other hand, is close to zero at low latitudes [*Dansgaard*, 1964; *Gonfiantini et al.*, 2001; *Rozanski et al.*, 1992]. Changes in seawater δD values at low latitudes are therefore primarily controlled by changes in the amount of precipitation and associated river runoff to the ocean.

Algal lipids have been shown to be excellent recorders of water D/H ratios in culture and in the field [*Englebrecht and Sachs*, 2005; *Sachse et al.*, 2004; 2006; *Sauer et al.*, 2001; *Zhang and Sachs*, 2007]. Measuring the δD value of lipid biomarkers has several advantages over that of bulk organic matter, including the ability to ascribe them to individual groups or species and the stability of carbon-bound hydrogen to exchange with water on geologic time scales [at least for <1 Ma, *Sessions et al.*, 2004].

The δD value of long-chain alkenones ($C_{37:2-3}$) ($\delta D_{alk}$), produced by haptophyte algae (mainly the coccolithophorid species *Emiliania huxleyi* and *Gephyrocapsa oceanica*), has been shown to reflect the δD value of the water in which the alkenones

were produced with near-perfection ($R^2$>0.99) [*Englebrecht and Sachs*, 2005; *Paul*, 2002; *Schouten et al.*, 2006] (Figure 3). A negative offset of ~225‰ is due to isotope fractionation during the synthesis of alkenones (initial deuterium depletion of the primary photosynthate of ~-171‰ [*Yakir and DeNiro*, 1990] plus additional fractionation during biosynthesis). This suggests that δD values measured in alkenones from marine sediments can be used to reconstruct past changes in freshwater supply to the ocean and hence precipitation and river runoff.

Two uncertainties with this approach are the potentially varying amounts of D/H fractionation during alkenone biosynthesis by different species or genera, and as yet unknown or poorly constrained environmental influences on D/H fractionation in alkenones [*Paul*, 2002; *Schouten et al.*, 2006; *Zhang and Sachs*, 2007]. If a succession of alkenone-producing species (or genera) occurs through time at a site, and different species discriminate against deuterium to varying degrees during alkenone biosynthesis, then a downcore change in $\delta D_{alk}$ values could arise in the absence of any change in water δD values. A similar case could be made for a change in light, nutrients, SST, SSS, etc., if any of those factors influence D/H fractionation during lipid synthesis.

To date little is known about the dependence of D/H fractionation in alkenones (or any other lipid) on species or environmental conditions. *Schouten et al.* [2006] reported $\delta D_{alk}$ values in *G. oceanica* that was ~30‰ lower than in *E. huxleyi* grown in batch cultures (Figure 3). In the same experiments, a positive correlation of isotope fractionation with salinity, amounting to ~3‰/salinity unit, was observed for both species, as was a negative correlation of D/H fractionation and growth rate. Conversely, no effect of growth rate on D/H fractionation in alkenones was observed by *Paul* [2002]. Moreover, results from chemostat (i.e., continuous culture) experiments with a marine diatom indicated no impact of growth rate on D/H fractionation in fatty acids [*Zhang and Sachs*, 2007]. Lastly, temperature changes had no effect on alkenone D/H fractionation in coccolithophorid batch cultures [*Schouten et al.*, 2006], but had a slight influence on D/H fractionation in lipids from green algal cultures [*Zhang and Sachs*, 2007].

At present, the largest influences on D/H fractionation during alkenone biosynthesis appear to be the species producing the alkenones and the salinity of the water. However, as discussed below (section 5), species changes are unlikely to mask our $\delta D_{alk}$ record, and salinity-dependant isotope fractionation would amplify the $\delta D_{alk}$ signal that is due to changes in the amount of precipitation and runoff to the Panama Basin. Other proxy data such as nannofossil abundances and $\delta^{18}O$ values of planktonic foraminifera are expected to elucidate these issues when they become available.

## 4 Material and Methods

### 4.1 Core locations

For the first downcore study of alkenone δD values we chose three cores from the Panama Basin in the tropical eastern Pacific that were obtained during R/V Knorr cruise 176-2 in February-March 2004 (http://www.marine.whoi.edu/kn_synop.nsf) (Figure 2). We sampled two short multi-cores, MC14 (4°50.81'N, 77°36.85'W, 884 m water depth, 32 cm long) and MC33 (4°39.99'N, 77°57.80'W, 2200 m water depth, 36 cm long), and the upper 800 cm of jumbo-piston core JPC32 (same location as MC33). The core sites are located off of western Colombia, close to the mouth of the Rio San Juan. Given the

salinity at our core site of 28.6 to 32.2 psu and an open ocean salinity of 34-34.5 psu [*Levitus et al.*, 1994], a simple concentration calculation suggests a freshwater contribution to the core site of 6-20.5%. The cores are therefore ideally located to sensitively monitor changes in river runoff and precipitation in the Colombian Andes, and to highlight their potential for a first test of the applicability of alkenone δD as hydrographic proxy. The proximity of the short cores to each other also permits testing the reproducibility of the δD signal recorded by alkenones.

### 4.2 Alkenone purification for D/H analysis

Multi-cores MC14 and MC33 were sampled at 1 or 2 cm and 1 to 4 cm intervals, respectively. Core JPC32 was sampled every 10 cm in the upper 8 m. Lipids were extracted from the freeze-dried sediment samples (3-9 g) with dichloromethane (DCM) at 100°C and 1000 psi on a Dionex ASE-200 pressurized fluid extractor (2x) and the total lipid extracts were combined and dried under a stream of $N_2$. Alkenone purification followed the protocol of *Englebrecht and Sachs* [2005] with slight modifications. Briefly, dry total lipid extracts were redissolved and hydrolyzed with 1N KOH in methanol:deionized water (3:1) at 60°C over night. Alkenones were extracted with 20 mL hexane (3x), back-extracted (1x), dehydrated over $Na_2SO_4$ and dried under a $N_2$ stream. The extracts were redissolved in a minimum amount of hexane and applied to a 9" Pasteur pipette containing 5 cm of activated silica gel (100-200 mesh). The samples were eluted with hexane (hydrocarbons), DCM:hexane (1:1) (alkenones), and methanol (polar compounds). Further purification was achieved by argentation column chromatography using a 9" pipette containing silver nitrate-coated silica gel and eluting the alkenones in ethyl ether. A final purification of alkenones was performed using a 9" pipette filled with 4 cm of activated silica gel (100-200 mesh) and eluting with DCM:hexane (1:1). When necessary, branched and cyclic molecules were removed from the alkenone fraction through urea adduction.

Alkenone purity, concentration and the relative abundance of $C_{37:3}$ and $C_{37:2}$ alkenones for SST estimation (see below) were measured on 5% aliquots of each sample using an Agilent 6890N gas chromatograph with a Chrompack CP-Sil-5 column (60 m by 0.32 mm i.d., 0.25 μm film thickness) and a programmable temperature vaporization inlet in solvent-vent mode. Helium was used as a carrier gas at a constant flow rate of 1.6mL/min and compounds were detected by flame-ionization. The oven was programmed from 110°C to 270°C at 40°C/min followed by a temperature increase of 2°C/min to 320°C, and an 18 minute isothermal period. Alkenones were quantified using co-injected *n*-hexatriacontane (*n*-$C_{36}$) as a quantitation standard. The samples contained a series of $C_{37}$-$C_{39}$ alkenones and showed a clean baseline in a large area around the alkenones where internal standards were introduced later for hydrogen isotope analysis. $C_{37}$-alkenone concentrations ranged from 0.15 to 1.7 μg/g dry sediment, which yielded 3 to 13 μg (average: 3.4 μg) of $C_{37}$ alkenones per sediment sample.

### 4.3 Hydrogen isotope analysis

Hydrogen isotope ratios were determined by isotope-ratio monitoring gas chromatography mass spectrometry (irmGC-MS) on a ThermoFinnigan Delta$^{plus}$ XP equipped with a Trace GC and Combustion III interface, using methods adapted from

*Sessions et al.* [1999] and *Sauer et al.* [2001]. The Trace GC was equipped with a PTV inlet operated in splitless mode, a 30-m DB-5 capillary column with 0.25 mm i.d. and 0.25 μm film thickness. With helium as carrier gas, the effluent from the GC entered the Combustion III interface, a graphite-lined tube held at 1400°C, where the sample was quantitatively pyrolyzed to graphite, $H_2$ and CO [*Burgoyne and Hayes*, 1998]. The hydrogen gas was then introduced to the mass spectrometer through an open split.

A correction factor for $H_3^+$ ions formed in the source was determined daily by measuring the (m/z-3)/(m/z-2) response of ten different concentrations of $H_2$ reference gas [*Sessions et al.*, 2001]. A low and stable value of 3-4 was typically achieved. The sensitivity of the instrument was monitored by injection of four pulses of $H_2$ reference gas at the beginning and two at the end of each run.

Two *n*-alkanes, *n*$C_{36}$ and *n*$C_{44}$, with known δD values that bracket the alkenone peaks in the chromatogram, were co-injected with each sample and used as isotopic standards for the computation of alkenone δD with IsoDat 2.0 software (ThermoFinnigan) (all isotope standards were obtained from Dr. Arndt Schimmelmann of the Biogeochemical Laboratories, Indiana University, Bloomington, IN, USA). For each measurement, ~1 μg $C_{37:2+3}$ alkenones were injected in 1 μL to obtain intensities of ~1000 mV, at which the results were most reproducible. Samples were run in duplicate or triplicate, alkenone concentrations permitting, with a typical standard deviation of less than 5‰. An isotope standard was measured after every 7-10 samples to ensure accuracy of alkenone δD values. The standard contained a series of 15 homologous *n*-alkanes (*n*$C_{16}$ to *n*$C_{30}$, mixture "Arndt-B"), with known δD values spanning a five-fold range in concentration and 214‰ in δD. The precision of δD measurements of this standard expressed as the average standard deviation of all measurements was ±3.7‰ (n = 79 injections) and the root-mean-square (RMS) error was 4‰ (n = 1027 measurements). All δD results are reported with reference to the VSMOW standard.

### 4.4 Alkenone SST estimation

We estimated sea surface temperatures (SST) from the unsaturation ratio of $C_{37:3}$ and $C_{37:2}$ alkenones using the $U_{37}^{K'}$ index ($U_{37}^{K'} = C_{37:2}/(C_{37:2}+C_{37:3})$), and the empirically derived $U_{37}^{K'}$-SST equation of *Prahl et al.* [1988] ($U_{37}^{K'} = 0.034T + 0.039$). This culture-based equation has been corroborated by an extensive field study of globally distributed core-top sediments [*Conte et al.*, 2006; *Müller et al.*, 1998] (600 core tops).

### 4.5 Stable oxygen isotopes

Hispid and smooth-shelled species of the benthic foraminifera *Uvigerina* were picked from the fraction >250 μm of core JPC32 for stable oxygen and carbon isotope analysis. Most of the analyses were performed on individual specimens. In the upper 400 cm of the core sample spacing was 20 cm. Below that depth it was 40cm. Analyses were carried out on a VG Prism mass spectrometer at the NOSAMS facility at Woods Hole Oceanographic Institution. Precision was better than 0.10‰ over the period of analyses as checked by routine runs of the NBS19 and other standards.

### 4.6 Age models

*Age models for multi-cores MC14 and MC33*

Age models for multi-cores MC14 and MC33 are based on $^{210}$Pb-dating. Seven to ten grams of dry sediment from the upper 20 cm and 14 cm of cores MC14 and MC33, respectively, were analysed for $^{210}$Pb on the gamma counter (Series 40 MCA, model GL2020) of the Department of Civil and Environmental Engineering at the Massachusetts Institute of Technology.

The decay of atmospherically produced $^{210}$Pb (excess or unsupported $^{210}$Pb, $^{210}Pb_{exs}$), measured in marine or lacustrine sediments, provides a measure for the rate of sedimentation and can be used to derive an age-depth correlation for sediment sequences over the past ~150 years. The total amount of $^{210}$Pb ($^{210}Pb_{total}$) in sediments has to be corrected for (supported) $^{210}$Pb supplied through the decay of $^{226}$Ra in the sediment. This was done by measuring the activity of $^{214}$Pb and subtracting it from $^{210}Pb_{total}$. Age-scales were then derived using the Constant Initial Concentration (CIC) model that assumes constant sedimentation rates and a zero age at the surface [*Goldberg*, 1962; *Krishnaswamy et al.*, 1971; *Turner and Delorme*, 1996].

The $^{210}Pb_{exs}$ depth-profiles of both cores (MC14, MC33) are shown in Figure 4a. Extrapolation of the age scales to the bottom of the cores at 32 cm (MC14) and 36 cm (MC33) indicates that MC14 spans the period from 1700 A.D. to the present and MC33 spans the period from 1600 A.D. to the present.

*Age model for JPC32*

The age model for core JPC32 is based on visual alignment of the benthic foraminiferal $\delta^{18}$O record from core JPC32 with the global $\delta^{18}$O stack of *Lisiecki and Raymo* [2005] (Figure 4b). According to this age model, the bottom of the studied section of JPC32 reaches 27 ka and our sampling interval of 10 cm corresponds to a mean temporal resolution of 380 yrs.

Accumulation rates for alkenone fluxes were calculated using dry bulk densities along the core.

## 5 Results and Discussion

### 6.1 Proof of concept: alkenone D/H changes over the past 400 years

Alkenone-derived SST estimates along MC14 and MC33 (Figure 5a) varied between 26.5 to 27.3°C and 26.3 to 27.2°C, respectively (Figure 5). The core-top SST estimates of 27°C (MC14) and 26.7°C (MC33) are consistent with the mean annual atlas SST at the core sites of 26.9°C [*Levitus and Boyer*, 1994]. The most notable features in the SST records are small declines in temperature (~0.4°C) at around 1822 A.D. (MC14) and 1867 A.D. (MC33), relatively constant SSTs subsequent to that drop and a temperature increase by some 0.7°C at 1897 AD (MC14) and at 1922 A.D. (MC33). Subsequently, temperatures in MC14 remained around 27.2°C until the present but dropped to 26.5°C in MC33 and remained slightly lower than in MC14.

Alkenone $\delta$D along cores MC14 and MC33, spanning the past three and four centuries, respectively, varied from -190 to -221‰ (MC14) and -195 to 219‰ (MC33) (Figure 5c). Prior to ~1900 A.D. both records show relatively similar values varying around a mean of -208‰ in core MC33 and slightly lower, around -210‰, in core MC14.

After ~1900 A.D. the records diverge: while $\delta D_{alk}$ values in MC14 decreased, reaching -221‰ at 1940 A.D., then increased again to a maximum value of -205‰ at 1988 A.D., $\delta D_{alk}$ values in core MC33 increased gradually to a maximum of -195‰ at 1986 A.D. Both records decrease in the 1990's to core-top values of -220‰ (MC14) and -205‰ (MC33), respectively (Figure 5d). Superimposed on these general trends are shorter-duration changes in both records that show obvious co-variations since ~1900. Two $\delta D_{alk}$ minima around 1940 and 1965 A.D. are followed by clear maxima around 1950 and 1986/87 A.D., and $\delta D_{alk}$ decreases of -10‰ (MC33) and -15‰ (MC14) since the late 1980's. Though the first two of these short-term minima in core MC33 are within the error of measurement, they are significant in the more highly resolved core MC14 and are supported by several data points.

*Discussion*

The $\delta D_{alk}$ records in MC14 and MC33 show similarities in absolute value, amplitude and timing of changes (Figure 5c, d). The consistently lower $\delta D_{alk}$ values in core MC14 compared to MC33 are expected from the closer proximity of that site to the large freshwater source of the San Juan River. Indeed, the surface salinity measured at the site of MC14 was 0.9 psu lower than at the site of MC33 in February 2004 (29.4 psu *vs.* 30.3 psu). Higher $\delta D_{alk}$ values in core MC33, on the other hand, are consistent with its location further offshore under a stronger influence of more saline, less D-depleted open-ocean surface waters.

In order to validate alkenone δD values in Colombian margin sediments as a hydrologic indicator, we compare our $\delta D_{alk}$ records to measured river discharge of Rio San Juan [*GRDC, The Global Runoff Data Centre*] and precipitation at a nearby site in Panama [Barro Colorado Island 9.17°N 79.84°W, Smithsonian Tropical Research Institute] (Figure 5b). (Unfortunately, records from Colombia only cover the period 1950-1985). Both $\delta D_{alk}$ records clearly co-vary with each other since 1920 A.D. ($r^2$ = 0.73, n = 7) and with precipitation in Panama over the time period of overlap (MC33: $r^2$ = 0.76, n = 7; MC14: $r^2$ = 0.3, n = 8. The 5pt moving average of the precipitation record was taken and sampled at the sample spacing of the MC records). For example, the gradual decrease in rainfall and river discharge prior to 1990 A.D. is accompanied by an increase in $\delta D_{alk}$ values, and the recent precipitation increase in Panama is reflected in our records by a $\delta D_{alk}$ decrease. Small inconsistencies between the $\delta D_{alk}$ records and precipitation changes in Panama are likely due to uncertainties in the age models of our cores. These results support the use of $\delta D_{alk}$ as a proxy for past changes in freshwater supply to the ocean and allow us to interpret $\delta D_{alk}$ changes in the Panama Basin in terms of hydrologic variations in tropical South America.

The $\delta D_{alk}$ divergence of our records at ~1900 A.D. indicates a salinity decrease at the inshore site of core MC14, and a trend towards higher salinity at the offshore site of core MC33 (Figure 5d). Core MC14 is located closer to the freshwater source of the San Juan and is likely to be more sensitive to changes in runoff and precipitation in Colombia than the more distal site of core MC33. An increase in precipitation and river discharge from the western Colombian Andes may have resulted from a northward shift of the mean position of the ITCZ and/or a strengthening of the westerly Chocó Jet, presumably

in association with increased meridional temperature gradients [*Poveda and Mesa*, 2000; *Poveda et al.*, 2001; *Restrepo and Kjerfve*, 2000].

## 5.1 Hydrologic and sea surface temperature changes over the past 27,000 years

### 5.1.1 Glacial-interglacial and Holocene changes

$U_{37}^{K'}$-SST values in core JPC32 averaged ca. 25°C during the LGM (18-23 ka) and recorded 26.5°C during the late Holocene (0-5 ka) (Figure 6c). The core-top SST of 27°C is in agreement with average $U_{37}^{K'}$-SSTs in the multi-cores of 26.8°C over the past 200 years and with the mean annual atlas SST at the core site of 26.9°C [*Levitus and Boyer*, 1994]. The mean glacial-interglacial SST change of ~1.3°C is within the range of amplitudes of 1.2-3°C previously reported for this time interval in the eastern tropical Pacific [*Benway et al.*, 2006; *Kienast et al.*, 2006; *Koutavas et al.*, 2002; *Lea et al.*, 2000; *Leduc et al.*, 2007].

The mid Holocene (7 ka) to present period is characterized by a trend of increasing SST of 1°C. This temperature increase is emerging as a tropical Pacific-wide feature that is documented in a growing number of, mainly alkenone-derived, SST records in the northern and southern tropics of the East and West Pacific [*Kienast et al.*, 2001; *Kienast et al.*, 2006; *Koutavas et al.*, 2002; *Koutavas and Lynch-Stieglitz*, 2003; *Koutavas et al.*, 2004; *Leduc et al.*, 2007]. The orbital precession pattern found in many tropical climate records [e.g., *Baker et al.*, 2001a; *Bush et al.*, 2002; *Cruz et al.*, 2005] cannot explain this Holocene SST feature since it appears in both hemispheres while precession imposes an opposite effect on insolation in the Northern and Southern Hemisphere. The temperature increase, however, coincides with an upward trend in annual mean insolation at mid to low latitudes (Figure 6). Studies of marine core-tops and sediment traps demonstrate that alkenones, despite significant differences in seasonal and interannual alkenone export, record mean annual SST [*Conte et al.*, 2006; *Müller et al.*, 1998; *Prahl et al.*, 2005]. It is therefore plausible that mean annual insolation changes may be imprinted on mid to low latitude SSTs as has previously been suggested for the time interval 47-23 ka [*Pahnke and Sachs*, 2006]. The amplitude of these insolation changes is small (~3.2W/m$^2$ at 5°N) relative to insolation changes at high-latitudes. However, low to mid-latitude warming may be reinforced by local greenhouse effects caused by increased water vapor and cloud formation over warm ocean areas. Pierrehumbert [1999] suggested that this mechanism may be active despite the negative feedback of radiative cooling caused by increased cloud cover. It is also instructive to consider that 3.5-4W/m$^2$ is the radiative increase accompanying a doubling of present atmospheric $CO_2$ levels [*Ramaswamy and I*, 2001], which is expected to cause global warming of 1.5-4.5°C.

Hydrogen isotope ratios measured on alkenones in core JPC32 varied between -222‰ and -183‰ (Figure 7b). The long-term trend over the past 27 ka indicates high $\delta D_{alk}$ values during the last glacial period and lower $\delta D_{alk}$ values during the Holocene. The core-top value of -204‰ is consistent with the $\delta D_{alk}$ value in multi-core MC33 at the same location that averaged -205‰ over the past 200 years. The mean glacial to late Holocene $\delta D_{alk}$ difference of 19‰ leaves an amplitude of ~11‰ after subtraction of glacial mean ocean D-enrichment of ~8‰, owing to isotopicallly depleted ice on the continents (Figure 7). Given a higher glacial mean ocean salinity of ~+1 [*Duplessy et al.*,

1991] and the apparent salinity effect on alkenone D/H fractionation of ~3‰/salinity unit [*Schouten et al.*, 2006], our data suggest 8‰ higher glacial $\delta D_{alk}$ values, presumably the result of diminished runoff. This is supported by the planktonic foraminiferal (*Globigerina bulloides*) stable oxygen isotope ($\delta^{18}O_{plk}$) record along our core that shows a glacial $\delta^{18}O$ enrichment of some 1.8‰ (LGM-Late Holocene, Figure 7). Correction for local SST using the $U^{K'}_{37}$-SST estimates along JPC32 and global seawater $\delta^{18}O$ [*Schrag et al.*, 2002; *Waelbroeck et al.*, 2002] suggests a glacial local seawater $\delta^{18}O$ ($\delta^{18}O_{sw}$) enrichment of ~+0.8‰. We are aware that combining proxies from two different proxy carriers to correct $\delta^{18}O_{plk}$ for local SST changes (alkenones, produced by coccolithophorids, and planktonic foraminifera) is not ideal and we therefore refrain from interpreting short-term $\delta^{18}O_{sw}$ changes. But the glacial-interglacial $\delta^{18}O_{sw}$ change of ~0.8‰ is substantial and cannot be entirely due to this shortcoming. The $\delta^{18}O_{plk}$ evidence therefore supports the glacial-interglacial change in surface water isotopic composition suggested by $\delta D_{alk}$. Given the linear relation of $\delta^{18}O$ and $\delta D$ [meteoric water line, *Rozanski et al.*, 1993], the observed glacial-interglacial $\delta^{18}O_{sw}$ change of ~0.8‰ should correspond to a $\delta D$ change of 6.5‰. This is close to our estimated glacial-interglacial $\delta D$ amplitude of 8‰ and thus further supports the reliable reflection of surface water isotopic changes in alkenones.

*Schouten et al.*'s [2006] culturing studies indicated that *G. oceanica* produced alkenones that were about 30‰ more depleted in deuterium relative to *E. huxleyi* (Figure 3a). Changes in the abundance of *G. oceanica* relative to *E. huxleyi* were quantified by *Martínez et al.* [2006] in ODP core 677B from 1.2°N in the Panama Basin (i.e., 3.2° of latitude south of our core site). During the LGM, *G. oceanica* abundances in core 677B were ~200% that of *E. huxleyi* abundances, while in the Holocene they dropped to ~50% [*Martínez et al.*, 2006] (Figure 8). The change in the relative abundance of the two species, absent any change in water $\delta D$, ought to have made LGM alkenones more depleted in deuterium relative to Holocene alkenones, the opposite of what we observe (Figure 8). Moreover, total alkenone concentrations and alkenone accumulation rates (calculated using dry bulk density) in JPC32, indicators of total coccolithophorid production, are consistently higher during the last glacial period compared to the Holocene (Figure 8). That is, if the general association of *G. oceanica* with high productivity [*Broerse et al.*, 2000; *Giraudeau*, 1992; *Martínez et al.*, 2006; *Ziveri et al.*, 1995] holds true in the Panama Basin, high glacial alkenone concentrations would suggest higher *G. oceanica* abundances and therefore lower $\delta D_{alk}$ values [*Schouten et al.*, 2006], opposite to what is observed. This suggests that the last glacial D-enrichment cannot be due to higher *E. huxleyi* relative to *G. oceanica* abundances, and that the observed glacial-to-interglacial $\delta D_{alk}$ decline must be considered a minimum change. Furthermore, neither the early $\delta D_{alk}$ decrease of ~30‰ that started at 17 ka, nor the other millennial scale $\delta D_{alk}$ changes of the last 27 ka have obvious counterparts in the alkenone accumulation rate record (Figure 8), making it unlikely that the observed alkenone D-depletions are due to transient increases of *G. oceanica* abundance relative to *E. huxleyi* abundance.

Salinity changes are more difficult to evaluate through time, but most likely would act to enhance the $\delta D_{alk}$ changes associated with freshwater fluxes to the ocean. *Schouten et al.* [2006] observed a positive correlation between salinity and $\delta D_{alk}$ values

of ~3‰/salinity unit [*Schouten et al.*, 2006], which would amplify the change in $\delta D_{alk}$ values that resulted from changes in runoff. For example, if freshwater fluxes to the Panama Basin increased, $\delta D_{alk}$ values would be expected to decrease both as a result of isotopically depleted runoff *and* as a result of lowered salinity. Thus, in areas of strong contrast between the δD value of precipitation and seawater, and high amounts of rainfall (e.g., in the tropics close to river deltas), any changes in alkenone δD values caused by species or growth rate variations are likely to be secondary to the first order effects caused by freshwater fluxes.

Another factor that can potentially account for changes in surface water and hence alkenone δD independent of the amount of precipitation and runoff, are variations in moisture source. Precipitation on the Caribbean side of the Isthmus of Panama is about 30‰ more D-enriched than on the Pacific side today [*IAEA*, 2006; *Lachniet and Patterson*, 2002] and decreases by ~30‰ in the course of cross-Isthmus transport from the Atlantic to the Pacific, resulting in no significant isotopic difference of Atlantic and Pacific-derived rainfall in the eastern tropical Pacific. A change in the moisture source from the Pacific to the Atlantic without a change in the amount of precipitation can therefore likely be ruled out as the cause of $\delta D_{alk}$ changes in our core.

The glacial alkenone D-enrichment and heavy $\delta^{18}O_{plk}$ values observed in core JPC32 therefore implies reduced precipitation and runoff to the Panama Basin at that time. Relatively drier conditions can be explained by a more southern position of the ITCZ and a colder glacial atmosphere, causing hydrologic conditions similar to those encountered today during boreal winter. That is, rainfall directly associated with ITCZ convection occurring south of its present location, resulted in reduced precipitation in the Panama Basin. More importantly, the westerly, moisture-laden Chocó Jet, the primary moisture source for Colombia today that is active during boreal summer when the ITCZ is well north of the equator, must have been weaker in response to a more southern position of the ITCZ. These changes are likely to have left a substantial imprint on surface water isotopic composition, and hence $\delta D_{alk}$ values in the Panama Basin.

A southern mean position of the ITCZ during the last glacial maximum period relative to the Holocene is at odds with two recent studies from 8°N in the Panama Basin that suggested no LGM-Holocene change in $\delta^{18}O_{sw}$, and thus precipitation [*Benway et al.*, 2006; *Leduc et al.*, 2007]. But it is in agreement with both terrestrial and marine paleorecords from the tropical Atlantic and South America [e.g., *Arz et al.*, 1998; *Baker et al.*, 2001b; *Bush and Colinvaux*, 1990; *Bush*, 2002; *Hooghiemstra and van der Hammen*, 1993; *Hughen et al.*, 1996; *Leyden*, 1985; *Mora and Pratt*, 2001; *Peterson et al.*, 2000; *Schmidt et al.*, 2004; *Wang et al.*, 2006; *Wang et al.*, 2004], as well as several model studies, that consistently suggest a southward shift of the ITCZ at times of high Northern Hemisphere ice volume and at times of reduced North Atlantic Deep Water (NADW) production [*Chiang and Bitz*, 2005; *Dahl et al.*, 2005; *Timmermann et al.*, 2005; *Timmermann et al.*, 2007b]. The disparity with salinity records from ~8°N in the eastern tropical Pacific are likely due to the complexity of precipitation sources in this area. While our site and western tropical South America likely receive most of their moisture from Pacific sources, the records from 8°N lie within a second area of maximum precipitation near Costa Rica (~5-9°N), that has been estimated to consist to 50% of Caribbean sources [*Benway and Mix*, 2004].

Some Holocene $\delta D_{alk}$ values in our record have large error bars due to low alkenone concentrations (see Figure 8b). Several trends, however, are apparent and robust. During the early Holocene, starting at ~9.8 ka, $\delta D_{alk}$ values increased by some 12‰ and remained around -200‰ until ~8 ka, followed by a decrease of 20-25‰ until ~5 ka. The subsequent $\delta D_{alk}$ increase of ~18‰ from 5-2.5 ka, suggests a drying trend that is consistent with drying in northern Venezuela [*Haug et al.*, 2001; *Tedesco and Thunell*, 2003] and a southward displacement of the ITCZ. The Cariaco Basin records indicate a minimum in precipitation around 3 ka and subsequent rapid increase that is also evident in our record as a decrease in $\delta D_{alk}$ values. The long-term D-depletion since 9 ka coincides with warming in the tropical Pacific (Figure 6) and is consistent with the association of warm SSTs with increased precipitation (e.g., at times of a northern mean position of the ITCZ).

### 5.1.2 The last glacial termination

The last deglaciation was characterized by an early and marked SST decrease by 1.5°C from ~17 to 14.5 ka, with minimum temperatures of 23.3°C at ~15.8-15.1 ka (Figure 6). This cold event is consistent with the cooling observed in another alkenone SST record from the eastern tropical Pacific at 0°N by *Kienast et al.* [2006] (Figure 6a) and coincides with cooling and a reduction in the AMOC in the North Atlantic Ocean in response to Heinrich event H1. The simultaneity of the cold anomaly in JPC32 with H1 is supported by its occurrence during the early deglaciation, when benthic $\delta^{18}O$ in our core, and hence global ice volume, was already decreasing. Other short-duration cold episodes in the glacial section of our record may also be associated with cold events in the North Atlantic, such as the one starting around 24-23.3 ka and lasting until ~22.3 ka (Figure 6), near the time of H2. Better age control is required to confirm this association.

At the time of the early deglacial cooling (H1), $\delta D_{alk}$ values decreased by ~30‰ starting at ~17 ka, and reached an initial minimum at ~13.5 ka (Figure 7). As discussed above, based on the alkenone accumulation record in JPC32 (Figure 8), changes in relative species abundance (*E. huxleyi* vs. *G. oceanica*) are unlikely to have caused the downcore $\delta D_{alk}$ variations.

Harsh climatic conditions characterized much of the Northern Hemisphere during H1 [*Hemming*, 2004] and the ITCZ is thought to have migrated southward [*Peterson et al.*, 2000; *Timmermann et al.*, 2005; *Timmermann et al.*, 2007b; *Wang et al.*, 2004]. A southward displacement of the ITCZ during H1, from an already southward-displaced glacial position, would have further suppressed Pacific moisture transport into tropical South America via the Chocó Jet. A concomitant $\delta D_{alk}$ decrease, however, suggests the opposite -- i.e., increased precipitation and runoff from Colombia.

Times of high-northern latitude cooling during H-events are associated with enhanced northeasterly trade winds [*Andreasen and Ravelo*, 1997; *Dahl et al.*, 2005; *Hughen et al.*, 1996] (Figure 9 and appendix) and tropical to southern-subtropical Atlantic warming (including the Cariaco Basin, the Caribbean and the Gulf of Mexico [*Flower et al.*, 2004; *Hüls and Zahn*, 2000; *Rühlemann et al.*, 1999; *Schmidt et al.*, 2004; *Weldeab et al.*, 2006]). These conditions are favorable for a strengthening of low-level winds crossing Central America from the Atlantic to the Pacific [Figure 9 and appendix, *Xie et al.*, 2007; *Xu et al.*, 2005]. The Panama Jet, that crosses the Isthmus of Panama from the east, develops today during boreal winter when the ITCZ is at its southernmost

position and northeasterly trade winds are strongest [*Mapes et al.*, 2003; *Xie et al.*, 2005]. It accounts for part of the moisture export from the Atlantic to the Pacific that is considered crucial for the maintenance of the Atlantic-Pacific salinity difference and thus the operation of the AMOC [*Baumgartner and Reichel*, 1975; *Hostetler and Mix*, 1999; *Stocker and Wright*, 1991; *Zaucker et al.*, 1994]. The total freshwater export from the Atlantic to the Pacific across Central America through the Papagayo, Tehuantepec and Panama topographic gaps has been estimated at 0.3 Sv (1Sv = $10^6$ $m^3$/s) [*Stocker and Wright*, 1991] and 0.32 Sv [*Xu et al.*, 2005].

An increase in moisture transport to the eastern tropical Pacific during North Atlantic H-events in conjunction with cold SSTs in the Panama Basin that are documented [Figure 6, *Kienast et al.*, 2006] could have caused the increase in freshwater supply indicated by our $\delta D_{alk}$ record (Figure 7). The Panama Jet leads to enhanced upwelling in the Panama Basin today [*Chelton et al.*, 2000; *Rodríguez-Rubio and Stuardo*, 2002], which should increase the impact of D–enriched subsurface waters on $\delta D_{alk}$ values while at the same time resulting in lower SSTs. Our observations from the deglaciation, however, show a cold event at ~17 ka and low and declining $\delta D_{alk}$ values relative to the LGM (Figure 7). The early deglacial $\delta D_{alk}$ decrease and other short-duration $\delta D_{alk}$ changes along JPC32 were therefore most likely caused by changes in freshwater supply to the Panama Basin rather than variations in upwelling.

*A regional coupled model experiment*

In order to test the scenario of increased Atlantic-Pacific moisture transport during H1, we used a regional ocean-atmosphere model (ROAM) [*Xie et al.*, 2007] to analyze the response of eastern tropical Pacific SST and precipitation to the shutdown of the AMOC forced by freshening of the northern North Atlantic. This experiment captures the cooling of the eastern tropical Pacific during H1 observed in paleotemperature records [*Kienast et al.*, 2006, this study Figure 6] (Figure 9; see appendix for a more detailed description of the model). The reduction in the annual cycle of SST over the eastern equatorial Pacific in the model results from anomalous northeasterly winds across Central America (Figure 9). Moreover, the convergence of strengthened northeasterly winds across Central America in the model is associated with increased precipitation in a narrow band in the eastern tropical Pacific (Figure 9b and appendix). Detailed analysis of the ROAM hosing experiment indicates that this precipitation increase is due to enhanced Atlantic freshwater export across Central America during H-events (I. Richter, pers. comm.). This is also indicated by other model simulations that produce enhanced Atlantic-Pacific moisture transport under El Niño-like conditions [*Schmittner et al.*, 2000; *Schmittner and Clement*, 2002]. Furthermore, paleoclimate records suggest an El Niño-like state during North Atlantic H-events [e.g., *Hong et al.*, 2005; *Koutavas et al.*, 2002; *Stott et al.*, 2002; *Zhang and Delworth*, 2005].

Our finding of increased precipitation in the eastern tropical Pacific (4.4°N) during H1 therefore appears plausible and is not in conflict with dry conditions in the Cariaco Basin [*Peterson et al.*, 2000] or at 8°N in the eastern tropical Pacific [*Benway et al.*, 2006; *Leduc et al.*, 2007].

## 6. Summary and Conclusions

We have used hydrogen isotope ratios in alkenones, produced by haptophyte algae, to document past hydrologic changes in the Panama Basin and western tropical South America. Two records covering the past 300-400 years demonstrate that alkenone δD values reflect variations in precipitation and runoff to the tropical eastern Pacific and can be used for paleo-hydrologic studies. A $\delta D_{alk}$ record spanning the past 27 ka indicates drier conditions during the last glacial period, likely caused by a southward shift of the ITCZ. The early deglaciation was marked by a 1.5°C sea-surface cooling (~17-14.5 ka), consistent with cooling found at 0°N in the eastern tropical Pacific [*Kienast et al.*, 2006]. This cooling coincided with the time of H1 in the North Atlantic and is consistent with the response of the eastern tropical Pacific to a reduction of the AMOC and associated strengthening of northeasterly trade winds in our ocean-atmosphere model. At the same time, a gradual $\delta D_{alk}$ decrease indicates an early deglacial increase in precipitation towards Holocene conditions. Increased rainfall is supported by our model that shows a narrow band of increased precipitation in the eastern tropical Pacific in response to a reduction of the AMOC and cooling in the North Atlantic (H1). The band of increased rainfall is associated with the convergence of anomalous northeasterly winds across Central America that are present year round and increase the Atlantic-to-Pacific moisture transport. This may have implications for the Atlantic-Pacific freshwater balance that is critical for the operation of the AMOC.

## Appendix

Regional coupled model experiment

A full-physics regional atmospheric model is coupled with an ocean general circulation model. The atmospheric model covers one third of the global tropics from 150$^o$W to 30$^o$W, 35$^o$S to 35$^o$N, with horizontal resolution 0.5$^o$ and 28 vertical levels. The ocean model covers the entire tropical Pacific from 35$^o$S to 35$^o$N, with horizontal resolution 0.5$^o$ and 30 vertical levels. The atmospheric and ocean models are restored to observations on the open boundaries, and are interactive in the eastern Pacific (east of 150$^o$W). The ocean model west of 150$^o$W is forced by observed atmospheric forcing while observed sea surface temperature (SST) is prescribed in the Atlantic to force the atmospheric model. The regional ocean-atmosphere model (ROAM) simulates the mean state and seasonal cycle of the eastern Pacific very well. In particular, the model reproduces the westerly Choco Jet that converges onto the Pacific coast of Colombia and creates a rainfall maximum exceeding 10 m/year (Figure 9a). For a detailed description of the model and its performance, readers are referred to *Xie et al*. [2007].

In response to an injection of fresh water in the high-latitude North Atlantic, as at the onset of Heinrich events, the cooling of the tropical North Atlantic is a common feature in different coupled general circulation models [GCMs, *Timmermann et al.*, 2007b]. The ROAM is used to investigate how this North Atlantic cooling induces changes in the tropical Pacific via the mountainous Central American Isthmus. Tropical North Atlantic SST is reduced by 2$^o$C to mimic the response there to water hosing. The prescribed cooling is spatially uniform north of 5$^o$N and tempered down to zero to 5$^o$S. The cooling causes atmospheric pressure to increase over the tropical North Atlantic and the increased pressure gradient with the Pacific drives anomalous northeasterly winds across Central America, a feature seen in all coupled GCMs in response to North Atlantic water hosing [*Timmermann et al.*, 2007b]. The anomalous northeasterly winds across Central America cause a reduction in the SST annual cycle over the equatorial eastern Pacific [*Xie et al.*, 2007].

Figure 9b shows the model response to North Atlantic cooling during July-August-September (JAS), the season when the atmospheric changes in wind and precipitation are the most pronounced since tropical North Atlantic SST is at its annual maximum and supports deep atmospheric convection. As a result, a unit change in SST there can induce a larger atmospheric response during JAS than in other seasons. Strong northeasterly wind anomalies of up to 8 m/s are found across Central America and cover a broad region over the eastern Pacific north of the equator. Negative SST anomalies are found on the coast from Panama to Ecuador, consistent with Alkenone SST observations during the Heinrich event [this study, *Kienast et al.*, 2006]. Precipitation decreases over much of the northeastern tropical Pacific, in line with paleo-salinity reconstructions from this area [*Benway et al.*, 2006; *Leduc et al.*, 2007]. But there is a narrow ribbon of increased rainfall to the south. This ribbon of increased rainfall is associated with the convergence of anomalous northeasterly winds across Central America and appears to be consistent with an intensified hydrological cycle during the Heinrich event as inferred from our $\delta D_{alk}$ record at JPC32. The anomalous cross-Central American winds are present year round and increase the Atlantic-to-Pacific transport of moisture.

**References**


Andreasen, D. J., and A. C. Ravelo (1997), Tropical Pacific Ocean thermocline depth reconstructions for the last glacial maximum, *Paleoceanography*, *12*(3), 395-414.

Arz, H. W., J. Patzold, and G. Wefer (1998), Correlated millennial-scale changes in surface hydrography and terrigenous sediment yield inferred from last-glacial marine deposits off northeastern Brazil, *Quaternary Research*, *50*(2), 157-166.

Baker, P. A., C. A. Rigsby, G. O. Seltzer, S. C. Fritz, T. K. Lowenstein, N. P. Bacher, and C. Veliz (2001a), Tropical climate changes at millennial and orbital timescales on the Bolivian Altiplano, *Nature*, *409*(6821), 698-701.

Baker, P. A., G. O. Seltzer, S. C. Fritz, R. B. Dunbar, M. J. Grove, P. M. Tapia, S. L. Cross, H. D. Rowe, and J. P. Broda (2001b), The history of South American tropical precipitation for the past 25,000 years, *Science*, *291*(5504), 640-643.

Baumgartner, A., and E. Reichel (1975), *The World Water Balance*, 179 pp., Elsevier.

Benway, H. M., and A. C. Mix (2004), Oxygen isotopes, upper-ocean salinity, and precipitation sources in the eastern tropical Pacific, *Earth and Planetary Science Letters*, *224*, 493-507.

Benway, H. M., A. C. Mix, and B. A. Haley (2006), Eastern Pacific Warm Pool paleosalinity and climate variability: 0–30 kyr, *Paleoceanography*, *21*(PA3008), doi:10.1029/2005PA001208.

Broerse, A. T. C., G.-J. A. Brummer, and J. E. V. Hinte (2000), Coccolithophore export production in response to monsoonal upwelling off Somalia (northwestern Indian Ocean), *Deep Sea Research Part II: Topical Studies in Oceanography*, *47*(9-11), 2179-2205.

Burgoyne, T. W., and J. M. Hayes (1998), Quantitative production of $H_2$ by pyrolysis of gas chromatographic effluents, *Analytical Chemistry*, *70*(24), 5136 -5141.

Bush, M. B., and P. A. Colinvaux (1990), A pollen record of a complete glacial cycle from lowland Panama, *Journal of Vegetation Science*, *1*(1), 105-118.

Bush, M. B., D. R. Piperno, P. A. Colinvaux, P. E. De Oliveira, L. A. Krissek, M. C. Miller, and W. E. Rowe (1992), A 14,300-yr paleoecological profile of a lowland tropical lake in Panama, *Ecological Monographs*, *62*(2), 251-275.

Bush, M. B. (2002), On the interpretation of fossil Poaceae pollen in the lowland humid neotropics, *Paleogeogr. Paleoclimatol. Paleoecol.*, *177*(1-2), 5-17.

Bush, M. B., M. C. Miller, P. E. De Oliveira, and P. A. Colinvaux (2002), Orbital forcing signal in sediments of two Amazonian lakes, *Journal of Paleolimnology*, *27*(3), 341-352.

Chelton, D. B., M. H. Freilich, and S. K. Esbensen (2000), Satellite Observations of the Wind Jets off the Pacific Coast of Central America. Part II: Regional Relationships and Dynamical Considerations, *Monthly Weather Review*, *128*(7), 2019-2043.

Chiang, J. C. H. (2005), Present-day climate variability in the tropical Atlantic: a model for paleoclimate changes?, in *The Hadley circulation: past, present, and future*, vol., edited by Diaz, H. F. and R. S. Bradley, pp. 465-488, Kluwer Academic Publishers.

Chiang, J. C. H., and C. M. Bitz (2005), Influence of high latitude ice cover on the marine Intertropical Convergence Zone, *Climate Dynamics*, *25*(5), 477-496.

Coe, M. T., and N. Olejniczak (1999), SAGE Global River Discharge Database. Available online at [http://www.sage.wisc.edu/riverdata/] from the Center for Sustainability and the Global Environment (SAGE), Gaylord Nelson Institute for Environmental Studies, University of Wisconsin-Madison, Madison, Wisconsin, USA.

Colinvaux, P. A., P. E. De Oliveira, J. E. Moreno, M. C. Miller, and M. B. Bush (1996), A Long Pollen Record from Lowland Amazonia: Forest and Cooling in Glacial Times, *Science*, *274*, 85-88.

Conte, M., M. A. Sicre, C. Rühlemann, J. C. Weber, S. Schulte, D. Schulz-Bull, and T. Blanz (2006), Global temperature calibrations of the alkenone unsaturation index ($U^{K'}_{37}$) in surface waters and comparsion with surface sediments, *Geochemistry Geophysics Geosystems*, *7*(Q02005), doi:10.1029/2005GC001054.

Cruz, F. W., S. J. Burns, I. Karmann, W. D. Sharp, M. Vuille, A. O. Cardoso, J. A. Ferrari, P. L. S. Dias, and O. Viana (2005), Insolation-driven changes in atmospheric circulation over the past 116,000 years in subtropical Brazil, *Nature*, *434*(7029), 63-66.

Dahl, K., A. Broccoli, and R. Stouffer (2005), Assessing the role of North Atlantic freshwater forcing in millennial scale climate variability: a tropical Atlantic perspective, *Climate Dynamics*, *24*(4), 325-346.

Dansgaard, W. (1964), Stable isotopes in precipitation, *Tellus*, *16*, 436-468.

Duplessy, J. C., L. Labeyrie, A. Juillet-Leclerc, F. Maitre, J. Duprat, and M. Sarnthein (1991), Surface salinity reconstruction of the North Atlantic Ocean during the last glacial maximum, *Oceanologica Acta*, *14*(4), 311-324.

Englebrecht, A. C., and J. P. Sachs (2005), Determination of sediment provenance at drift sites using hydrogen isotopes and unsaturation ratios in alkenones, *Geochimica et Cosmochimica Acta*, *69*(17), 4253-4265.

Flower, B. P., D. W. Hastings, H. W. Hill, and T. M. Quinn (2004), Phasing of deglacial warming and laurentide ice sheet meltwater in the Gulf of Mexico, *Geology*, *32*(7), 597-600.

Gat, J. R. (1996), Oxygen and hydrogen isotopes in the hydrologic cycle, *Annual Review of Earth and Planetary Sciences*, *24*, 225-262.

Giraudeau, J. (1992), Distribution of Recent nannofossils beneath the Benguela system: Southwest African continental margin, *Marine Geology*, *108*(2), 219-237.

Goldberg, E. D. (1962), Geochronology with $^{210}$Pb, in *Proceedings of the Symposium on Radioactive Dating*, edited, pp. 121–131, International Atomic Energy Agency (IEAE), Vienna.

Gonfiantini, R., M. A. Roche, J. C. Olivry, J. C. Fontes, and G. M. Zuppi (2001), The altitude effect on the isotopic composition of tropical rains, *Chemical Geology*, *181*(1-4), 147-167.

GRDC, The Global Runoff Data Centre, D - 56002 Koblenz, Germany, http://grdc.bafg.de.

Haug, G. H., K. A. Hughen, D. M. Sigman, L. C. Peterson, and U. Röhl (2001), Southward migration of the Intertropical Convergence Zone through the Holocene, *Science*, *293*, 1304-1308.

Hemming, S. R. (2004), Heinrich events: Massive late pleistocene detritus layers of the North Atlantic and their global climate imprint, *Reviews of Geophysics*, *42*(1).

Hong, Y. T., B. Hong, Q. H. Lin, Y. Shibata, M. Hirota, Y. X. Zhu, X. T. Leng, Y. Wang, H. Wang, and L. Yi (2005), Inverse phase oscillations between the East Asian and Indian Ocean summer monsoons during the last 12 000 years and paleo-El Niño, *Earth and Planetary Science Letters*, *231*(3-4), 337-346.

Hooghiemstra, H., and T. van der Hammen (1993), Late quaternary vegetation history and paleoecology of Laguna Pedro Palo (subandean forest belt, Eastern Cordillera, Colombia), *Review of Palaeobotany and Palynology*, *77*(3-4), 235-262.

Hostetler, S. W., and A. C. Mix (1999), Reassessment of ice-age cooling of the tropical ocean and atmosphere, *Nature*, *399*, 673-676.

Hughen, K. A., J. T. Overpeck, L. C. Peterson, and S. Trumbore (1996), Rapid climate changes in the tropical Atlantic region during the last deglaciation, *Nature*, *380*, 51-54.

Hüls, M., and R. Zahn (2000), Millennial-scale sea surface temperature variability in the western tropical North Atlantic from planktonic foraminiferal census counts, *Paleoceanography*, *15*(6), 659-678.

IAEA (2006), Isotopes in precipitation, edited, Isotope Hydrology Information System (ISOHIS), The ISOHIS Database, accessible at: http://isohis.iaea.org.

Kienast, M., S. Steinke, K. Stattegger, and S. E. Calvert (2001), Synchronous tropical South China Sea SST change and Greenland warming during deglaciation, *Science*, *291*, 2132-2134.

Kienast, M., S. S. Kienast, S. E. Calvert, T. I. Eglinton, G. Mollenhauer, R. Francois, and A. C. Mix (2006), Eastern Pacific cooling and Atlantic overturning circulation during the last deglaciation, *Nature*, *443*, 846-849.

Koutavas, A., J. Lynch-Stieglitz, T. M. Marchitto, Jr., and J. P. Sachs (2002), El Niño-like pattern in ice age tropical Pacific sea surface temperature, *Science*, *297*, 226-230.

Koutavas, A., and J. Lynch-Stieglitz (2003), Glacial-interglacial dynamics of the eastern equatorial Pacific cold tongue-Intertropical Convergence Zone system reconstructed from oxygen isotope records, *Paleoceanography*, *18*(4), 1089, doi: 1010.1029/2003PA000894.

Koutavas, A., J. P. Sachs, L. D. Stott, J. Lynch-Stieglitz, and P. B. de Menocal (2004), Holocene sea surface temperature trends in the equatorial Pacific Ocean, paper presented at 1st International CLIVAR Conference., Baltimore, MD, USA.

Krebs, U., and A. Timmermann (2007), Tropical air-sea interactions accelerate the recovery of the Atlantic Meridional Overturning Circulation after a major shutdown, *Climate Dynamics*, *accepted*.

Krishnaswamy, S., D. Lal, J. M. Martin, and M. Meybeck (1971), Geochronology of lake sediments, *Earth and Planetary Science Letters*, *11*, 407-414.

Lachniet, M. S., and W. P. Patterson (2002), Stable isotope values of Costa Rican surface waters, *Journal of Hydrology*, *260*(1-4), 135-150.

Lea, D. W., D. K. Pak, and H. J. Spero (2000), Climate impact of late Quaternary Equatorial Pacific sea surface temperature variations, *Science*, *289*(5485), 1719-1724.

Leduc, G., L. Vidal, K. Tachikawa, F. Rostek, C. Sonzogni, L. Beaufort, and E. Bard (2007), Moisture transport across Central America as a positive feedback on abrupt climatic changes, *Nature*, *445*, 908-911.

Levitus, S., and T. P. Boyer (1994), *World Ocean Atlas 1994: Temperature*, 117 pp., U.S. Department of Commerce, Washington, D.C.

Levitus, S., R. Burgett, and T. P. Boyer (1994), *World Ocean Atlas 1994: Salinity*, 99 pp., U.S. Department of Commerce, Washington, D.C.

Leyden, B. W. (1985), Late Quaternary aridity and Holocene moisture fluctuations in the Lake Valencia Basin, Venezuela, *Ecology*, *66*(4), 1279-1295.

Lisiecki, L. E., and M. E. Raymo (2005), A Pliocene-Pleistocene stack of 57 globally distributed benthic $\delta^{18}O$ records, *Paleoceanography*, *20*(1).

Mapes, B. E., T. T. Warner, M. Xu, and A. J. Negri (2003), Diurnal patterns of rainfall in northwestern South America. Part I: Observations and context, *Monthly Weather Review*, *131*(5), 799-812.

Martínez, J. I., D. Rincon, Y. Yokoyama, and T. Barrows (2006), Foraminifera and coccolithophorid assemblage changes in the Panama Basin during the last deglaciation: Response to sea-surface productivity induced by a transient climate change, *Palaeogeography, Palaeoclimatology, Palaeoecology*, *234*(1), 114-126.

Maslin, M. A., and S. J. Burns (2000), Reconstruction of the Amazon Basin effective moisture availability over the past 14,000 years, *Science*, *290*(5500), 2285-+.

Mayle, F. E., D. J. Beerling, W. D. Gosling, and M. B. Bush (2004), Responses of Amazonian ecosystems to climatic and atmospheric carbon dioxide changes since the last glacial maximum, *Philosophical Transactions of the Royal Society of London. Series B*, *359*(1443), 499-514.

Mora, G., and L. M. Pratt (2001), Isotopic evidence for cooler and drier conditions in the tropical Andes during the last glacial stage, *Geology*, *29*(6), 519-522.

Müller, P. J., G. Kirst, G. Ruhland, I. von Storch, and A. Rosell-Mele (1998), Calibration of the alkenone paleotemperature index $U^{k'}_{37}$ based on core-tops from the eastern South Atlantic and the global ocean (60°N-60°S), *Geochimica et Cosmochimica Acta*, *62*(10), 1757–1772.

NCEP/NCAR Reanalysis Project, http://www.cdc.noaa.gov/cdc/reanalysis/index.html.

Pahnke, K., and J. P. Sachs (2006), Sea surface temperatures of southern midlatitudes 0–160 kyr B.P., *Paleoceanography*, *21*(PA2003), doi:10.1029/2005PA001191.

Paul, H. A. (2002), Application of Novel Stable Isotope Methods to Reconstruct Paleoenvironments: Compound-Specific Hydrogen Isotopes and Pore-Water Oxygen Isotopes, Swiss Federal Institute of Technology, Zürich.

Peterson, L. C., G. H. Haug, K. A. Hughen, and U. Röhl (2000), Rapid changes in the hydrologic cycle of the tropical Atlantic during the last glacial, *Science*, *290*, 1947-1951.

Peterson, L. C., and G. H. Haug (2006), Variability in the mean latitude of the Atlantic Intertropical Convergence Zone as recorded by riverine input of sediments to the Cariaco Basin (Venezuela), *Paleogeogr. Paleoclimatol. Paleoecol.*, *234*(1), 97-113.

Pierrehumbert, R. T. (1999), Subtropical water vapor as a mediator of rapid global climate change, in *Mechanisms of Global Climate Change at Millennial Time Scales*, *Geophysical Monograph*, vol. 112, edited by Clark, P. U., R. S. Webb and

L. Keigwin, pp. 339-360, American Geophysical Union, Washington, DC, United States.

Poveda, G., and O. J. Mesa (1997), Feedbacks between hydrological processes in tropical South America and large-scale ocean-atmospheric phenomena, *Journal of Climate*, *10*(10), 2690-2702.

Poveda, G., and O. J. Mesa (2000), On the existence of Lloro (the rainiest locality on earth): Enhanced ocean-land-atmosphere interaction by a low-level jet, *Geophysical Research Letters*, *27*(11), 1675-1678.

Poveda, G., A. Jaramillo, M. M. Gil, N. Quiceno, and R. I. Mantilla (2001), Seasonality in ENSO-related precipitation, river discharges, soil moisture, and vegetation index in Colombia, *Water Resources Research*, *37*(8), 2169-2178.

Prahl, F. G., L. A. Muehlhausen, and D. L. Zahnle (1988), Further evaluation of long-chain alkenones as indicators of paleoceanographic conditions, *Geochimica et Cosmochimica Acta*, *52*(9), 2303-2310.

Prahl, F. G., B. N. Popp, D. M. Karl, and M. A. Sparrow (2005), Ecology and biogeochemistry of alkenone production at Station ALOHA, *Deep Sea Research Part I: Oceanographic Research Papers*, *52*(5), 699-719.

Ramaswamy, V., and a. m. o. I. W. G. I (2001), Radiative forcing of climate change, Cambridge University Press.

Restrepo, J. D., and B. Kjerfve (2000), Water discharge and sediment load from the western slopes of the Colombian Andes with focus on Rio San Juan, *The Journal of Geology*, *108*, 17-33.

Restrepo, J. D., and B. Kjerfve (2002), The San Juan Delta, Colombia: tides, circulations, and salt dispersion, *Continental Shelf Research*, *22*(8), 1249-1267.

Rodríguez-Rubio, E., and J. Stuardo (2002), Variability of photosynthetic pigments in the Colombian Pacific Ocean and its relationship with the wind field using ADEOS-I data, *Proceedings of the Indian Academy of Sciences*, *11*(3), 227-236.

Rodríguez-Rubio, E., W. Schneider, and R. Abarca del Río (2003), On the seasonal circulation within the Panama Bight derived from satellite observations of wind, altimetry and sea surface temperature, *Geophysical Research Letters*, *30*(7), doi:10.1029/2002GL016794.

Rozanski, K., L. Araguás-Araguás, and R. Gonfiantini (1992), Relation between long-term trends of oxygen-18 isotope composition of precipitation and climate, *Science*, *258*, 981-985.

Rozanski, K., L. Araguas-Araguas, and R. Gonfiantini (1993), Isotopic patterns in modern global precipitation, in *Climate Change in Continental Isotopic Records*, vol. 78, edited by Swart, P. K., et al., pp. 1-37, AGU Geophys. Monogr.

Rühlemann, C., S. Mulitza, P. J. Müller, G. Wefer, and R. Zahn (1999), Warming of the tropical Atlantic Ocean and slowdown of thermohaline circulation during the last deglaciation, *Nature*, *402*, 511-514.

Sachse, D., J. Radke, and G. Gleixner (2004), Hydrogen isotope ratios of recent lacustrine sedimentary n-alkanes record modern climate variability, *Geochimica et Cosmochimica Acta*, *68*(23), 4877-4889.

Sachse, D., J. Radke, and G. Gleixner (2006), δD values of individual n-alkanes from terrestrial plants along a climatic gradient - Implications for the sedimentary biomarker record, *Organic Geochemistry*, *37*(4), 469-483.

Sauer, P. E., T. I. Eglinton, J. M. Hayes, A. Schimmelmann, and A. L. Sessions (2001), Compound-specific D/H ratios of lipid biomarkers from sediments as a proxy for environmental and climatic conditions, *Geochimica et Cosmochimica Acta*, *65*(2), 213-222.

Schmidt, M. W., H. J. Spero, and D. W. Lea (2004), Links between salinity variation in the Caribbean and North Atlantic thermohaline circulation, *Nature*, *428*, 160 - 163.

Schmittner, A., C. Appenzeller, and T. F. Stocker (2000), Enhanced Atlantic freshwater export during El Niño, *Geophysical Research Letters*, *27*(8), 1163-1166.

Schmittner, A., and A. C. Clement (2002), Sensitivity of the thermohaline circulation to tropical and high latitude freshwater forcing during the last glacial-interglacial cycle, *Paleoceanography*, *17*(2), 10.1029/2000PA000591.

Schouten, S., J. Ossebaar, K. Schreiber, M. V. M. Kienhuis, G. Langer, A. Benthien, and J. Bijma (2006), The effect of temperature, salinity and growth rate on the stable hydrogen isotopic composition of long chain alkenones produced by *Emiliania huxleyi* and *Gephyrocapsa oceanica*, *Biogeosciences*, *3*, 113-119.

Schrag, D. P., J. F. Adkins, K. McIntyre, J. L. Alexander, D. A. Hodell, C. D. Charles, and J. F. McManus (2002), The oxygen isotopic composition of seawater during the Last Glacial Maximum, *Quaternary Science Reviews*, *21*, 331-342.

Sessions, A. L., T. W. Burgoyne, A. Schimmelmann, and J. M. Hayes (1999), Fractionation of hydrogen isotopes in lipid biosynthesis, *Organic Geochemistry*, *30*(9), 1193-1200.

Sessions, A. L., T. W. Burgoyne, and J. M. Hayes (2001), Correction of $H_3^+$ contributions in hydrogen isotope ratio monitoring mass spectrometry, *Analytical Chemistry*, *73*(2), 192-199.

Sessions, A. L., S. P. Sylva, R. E. Summons, and J. M. Hayes (2004), Isotopic exchange of carbon-bound hydrogen over geologic timescales, *Geochimica et Cosmochimica Acta*, *68*(7), 1545-1559.

Small, R. J. O., S. P. de Szoeke, and S.-P. Xie (2007 in press), The Central American mid-summer drought: Regional aspects and large scale forcing, *Journal of Climate*.

Stocker, T. F., and D. G. Wright (1991), Rapid transitions of the ocean's deep circulation induced by changes in surface water fluxes, *Nature*, *351*, 729-732.

Stocker, T. F., and S. J. Johnsen (2003), A minimum thermodynamic model for the bipolar seesaw, *Paleoceanography*, *18*(4), 1087, doi: 1010.1029/2003PA000920.

Stott, L., K. Cannariato, R. Thunell, G. H. Haug, A. Koutavas, and S. Lund (2004), Decline of surface temperature and salinity in the western tropical Pacific Ocean in the Holocene epoch, *Nature*, *431*(7004), 56-59.

Stott, L. D., C. Poulsen, S. Lund, and R. Thunell (2002), Super ENSO and global climate oscillations at millennial time scales, *Science*, *297*, 222-226.

Stouffer, R. J., D. Seidov, and B. J. Haupt (2007), Climate response to external sources of freshwater: North Atlantic *versus* the Southern Ocean, *Journal of Climate*, *23*(3), 436-448.

Stute, M., J. F. Clark, P. Schlosser, W. S. Broecker, and G. Bonani (1995), A 30,000-Yr Continental Paleotemperature Record Derived from Noble-Gases Dissolved in

Groundwater from the San-Juan Basin, New-Mexico, *Quaternary Research*, *43*(2), 209-220.
Tedesco, K., and R. Thunell (2003), High resolution tropical climate record for the last 6,000 years, *Geophysical Research Letters*, *30*(17), doi: 10.1029/2003GL017959.
Timmermann, A., F. B. Justino, F.-F. Jin, and H. Goosse (2004), Surface temperature control in the North and tropical Pacific during the last glacial maximum, *Climate Dynamics*, *23*, 353-370.
Timmermann, A., U. Krebs, F. Justino, H. Goosse, and T. S. Ivanochko (2005), Mechanisms for millennial-scale global synchronization during the last glacial period, *Paleoceanography*, *20*(PA4008), doi: 10.1029/2004PA001090.
Timmermann, A., S. Lorenz, S.-I. An, A. Clement, and S.-P. Xie (2007a), The effect of orbital forcing on the mean climate and variability of the tropical Pacific, *Journal of Climate, accepted*.
Timmermann, A., Y. Okumura, S.-I. An, A. Clement, B. Dong, E. Guilyardi, A. Hu, J. Jungclaus, U. Krebs, and M. Renold (2007b), The influence of a shutdown of the Atlantic meridional overturning circulation on ENSO, *Journal of Climate, in press*.
Turner, L. J., and L. D. Delorme (1996), Assessment of $^{210}$Pb data from Canadian lakes using the CIC and CRS models, *Environmental Geology*, *28*(2), 78-87.
Turney, C. S. M., A. P. Kershaw, S. C. Clemens, N. Branch, P. T. Moss, and L. K. Fifield (2004), Millennial and orbital variations of El Niño/Southern Oscillation and high-latitude climate in the last glacial period, *Nature*, *428*(6980), 306-310.
Vernekar, A. D., B. P. Kirtman, and M. J. Fennessy (2003), Low-level jets and their effects on the South American summer climate as simulated by the NCEP Eta Model, *Journal of Climate*, *16*(2), 297–311.
Waelbroeck, C., L. Labeyrie, E. Michel, J. C. Duplessy, J. F. McManus, K. Lambeck, E. Balbon, and M. Labracherie (2002), Sea-level and deep water temperature changes derived from benthic foraminifera isotopic records, *Quaternary Science Reviews*, *21*, 295-305.
Wang, X., A. S. Auler, R. L. Edwards, H. Cheng, E. Ito, and M. Solheid (2006), Interhemispheric anti-phasing of rainfall during the last glacial period, *Quaternary Science Reviews*, *25*(23-24), 3391-3403.
Wang, X. F., A. S. Auler, R. L. Edwards, H. Cheng, P. S. Cristalli, P. L. Smart, D. A. Richards, and C. C. Shen (2004), Wet periods in northeastern Brazil over the past 210 kyr linked to distant climate anomalies, *Nature*, *432*(7018), 740-743.
Weldeab, S., R. R. Schneider, and M. Kolling (2006), Deglacial sea surface temperature and salinity increase in the western tropical Atlantic in synchrony with high latitude climate instabilities, *Earth and Planetary Science Letters*, *241*(3-4), 699-706.
Xie, S.-P., and J. A. Carton (2004), Tropical Atlantic variability: Patterns, mechanisms, and impacts, in *Earth Climate: The Ocean-Atmosphere Interaction, Geophysical Monograph*, vol. 147, edited by Wang, C., S.-P. Xie and J. A. Carton, pp. 121-142, AGU, Washington D.C.
Xie, S.-P., T. Miyama, Y. Wang, H. Xu, S. P. de Szoeke, R. J. Small, K. J. Richards, T. Mochizuki, and T. Awaji (2007), A regional ocean-atmosphere model for eastern

Pacific climate: Towards reducing tropical biases, *Journal of Climate*, *20*, 1504-1522.
Xie, S. P., H. M. Xu, W. S. Kessler, and M. Nonaka (2005), Air-sea interaction over the eastern Pacific warm pool: Gap winds, thermocline dome, and atmospheric convection, *Journal of Climate*, *18*(1), 5-20.
Xu, H., S. P. Xie, Y. Wang, and R. J. Small (2005), Effects of Central American mountains on the eastern Pacific winter ITCZ and moisture transport, *Journal of Climate*, *18*, 3856-3873.
Yakir, D., and M. J. DeNiro (1990), Oxygen and hydrogen isotope fractionation during cellulose metabolism in *Lemna gibba L*, *Plant Physiology*, *93*, 325-332.
Zaucker, F., T. F. Stocker, and W. S. Broecker (1994), Atmospheric freshwater fluxes and their effect on the global thermohaline circulation, *Journal of Geophysical Research*, *99*(C6), 12443-12458.
Zhang, R., and T. L. Delworth (2005), Simulated tropical response to a substantial weakening of the Atlantic thermohaline circulation, *Journal of Climate*, *18*(12), 1853-1860.
Zhang, Z., and J. P. Sachs (2007), Hydrogen isotope fractionation in freshwater algae: I. Variations among lipids and species, *Organic Geochemistry*, *38*(4), 582-608.
Ziveri, P., R. C. Thunell, and D. Rio (1995), Export production of coccolithophores in an upwelling region: Results from San Pedro Basin, Southern California Borderlands, *Marine Micropaleontology*, *24*(3-4), 335-358.

**Figures**

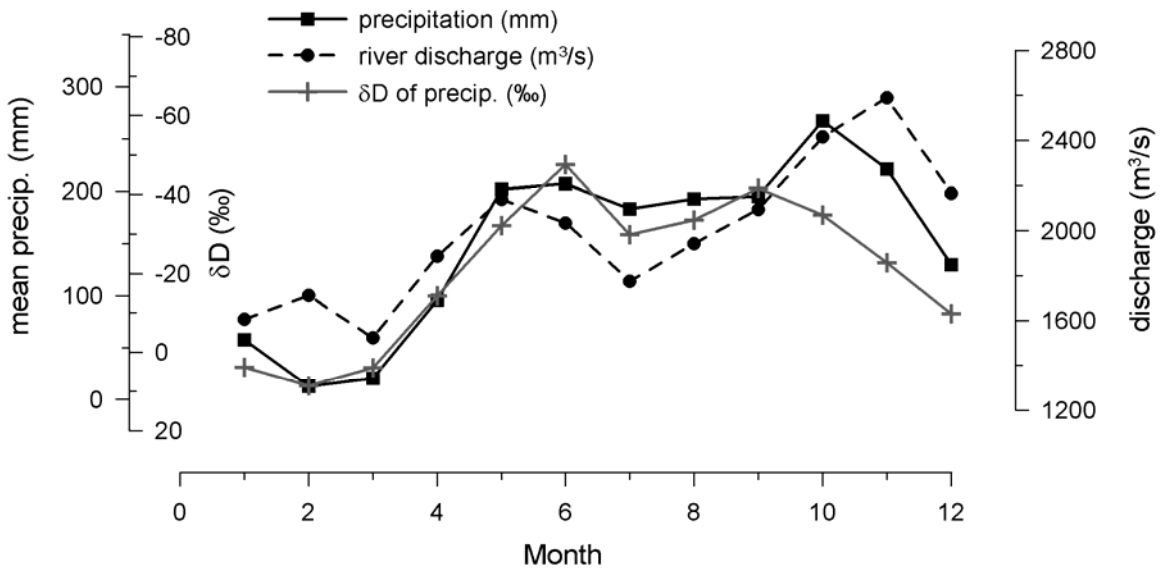


**Figure 1:** Annual changes in river discharge [*Coe and Olejniczak*, 1999], precipitation and δD of precipitation in Panama [*IAEA*, 2006] (Note inverted δD axis).

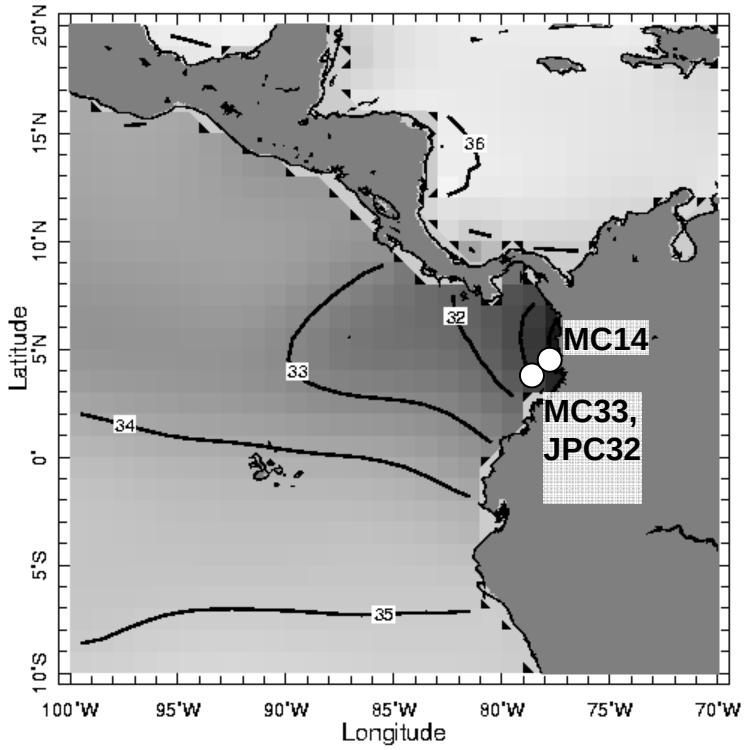


**Figure 2:** Core locations on a map of mean annual sea surface salinity [*Levitus et al.*, 1994].

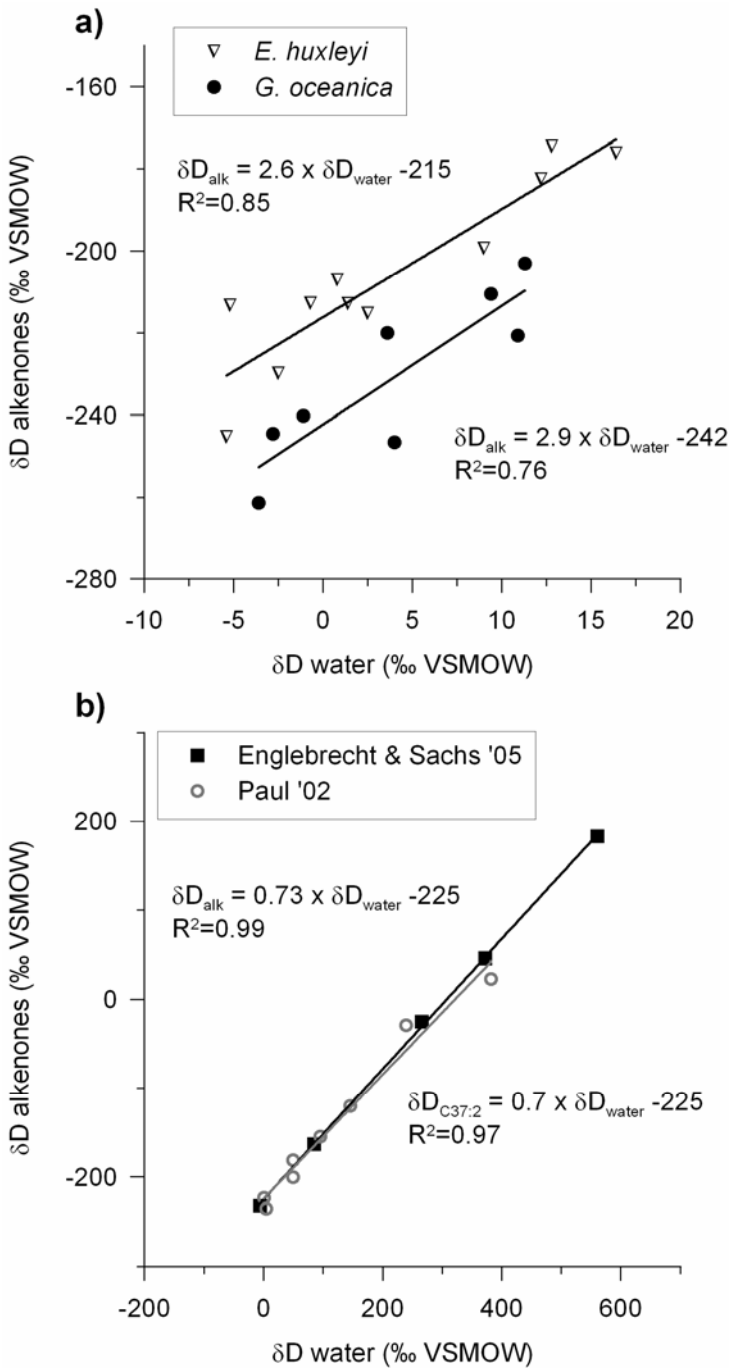


**Figure 3:** Alkenone δD *versus* water δD of culture studies. a) $\delta D_{alk}$ *vs.* $\delta D_{water}$ for *E. huxleyi* and *G. oceanica* [*Schouten et al.*, 2006]. b) same as in a) but culture data from *Englebrecht and Sachs* [2005] (squares) and *Paul* [2002] (circles) for *E. huxleyi*.

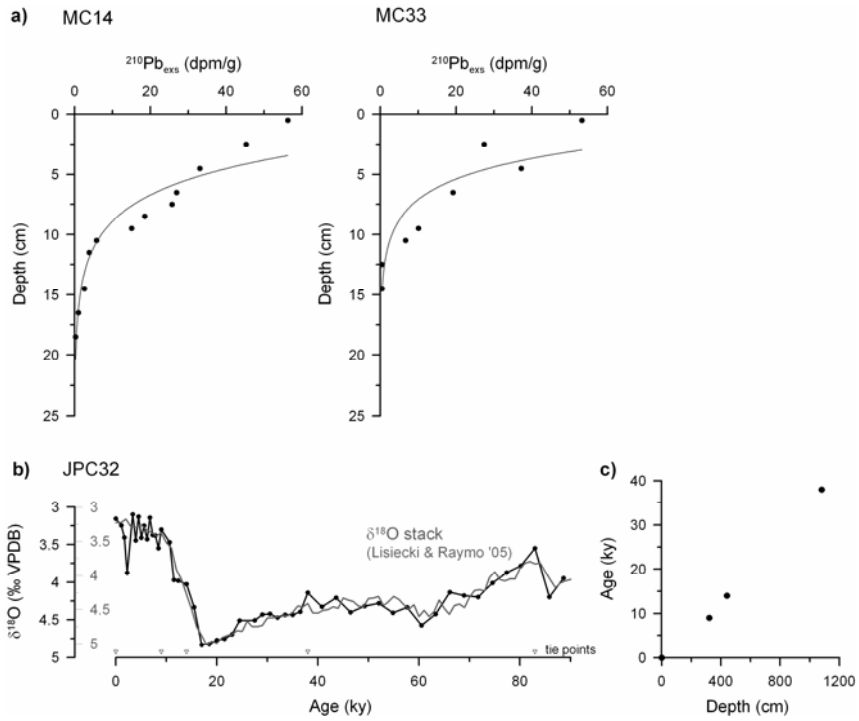


**Figure 4:** Age models for the multi-cores (MC14, MC33) and JPC32. a) $^{210}$Pb profiles for MC14 and MC33. b) Benthic foraminiferal (*Uvigerina*) $\delta^{18}$O record of core JPC32 over the past 90 ka compared with the global benthic $\delta^{18}$O stack of *Lisiecki and Raymo* [2005], arrows mark tie points used to align the benthic record of JPC32 to the global $\delta^{18}$O stack. c) Age-depth plot for JPC32.

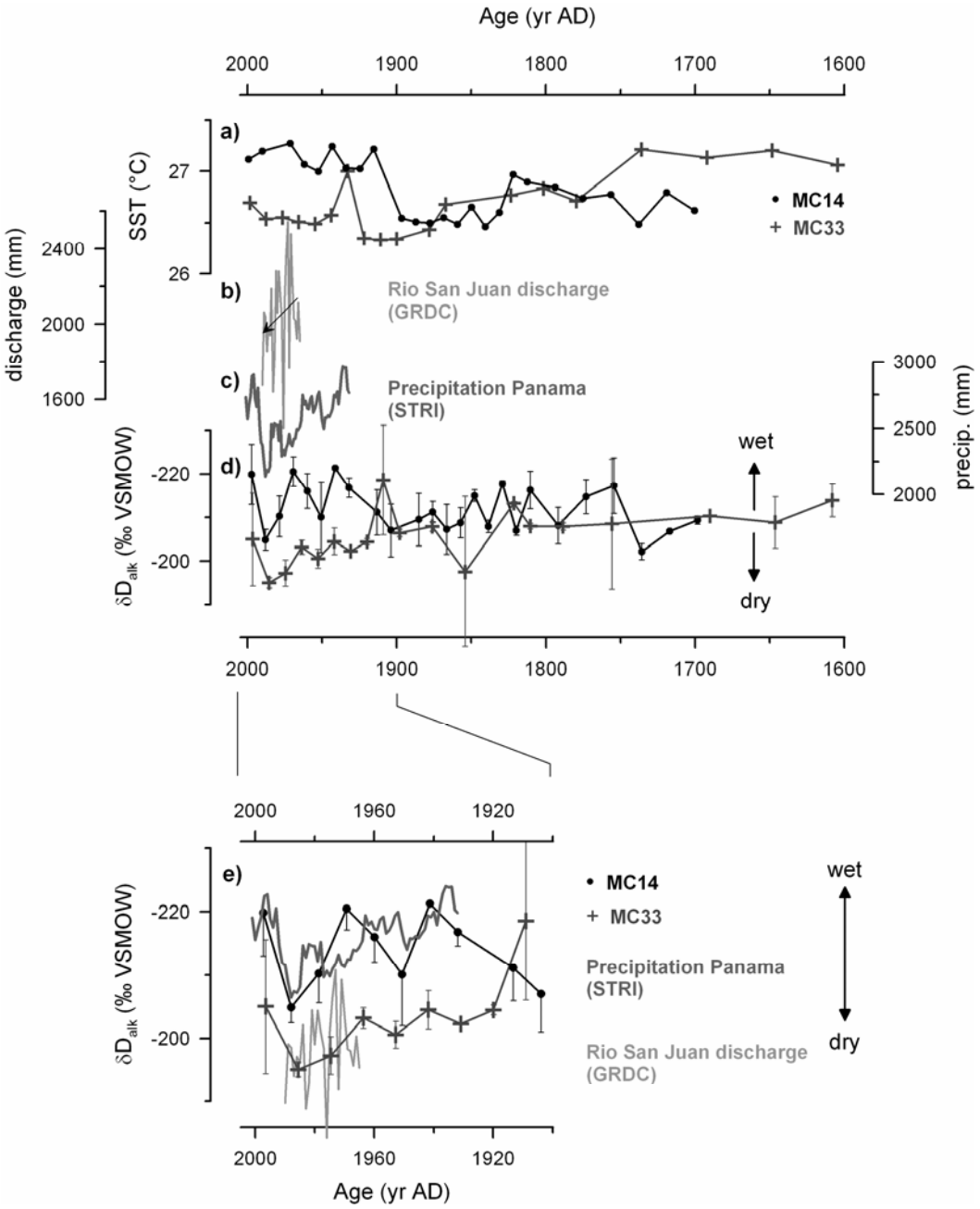


**Figure 5:** $U_{37}^{K'}$-derived SST and $\delta D_{alk}$ records of multi-cores MC14 (circles) and MC33 (crosses). a) SST and d) $\delta D_{alk}$ records over the past 300 and 400 years compared to b) mean annual discharge of Rio San Juan [*GRDC, The Global Runoff Data Centre*] and c) an instrumental record of precipitation in Panama (7-point running mean) [*STRI, Smithsonian Tropical Research Institute*]. e) Detailed view of the past ~100 years that are covered by the precipitation and discharge records. Note inverted δD axes.

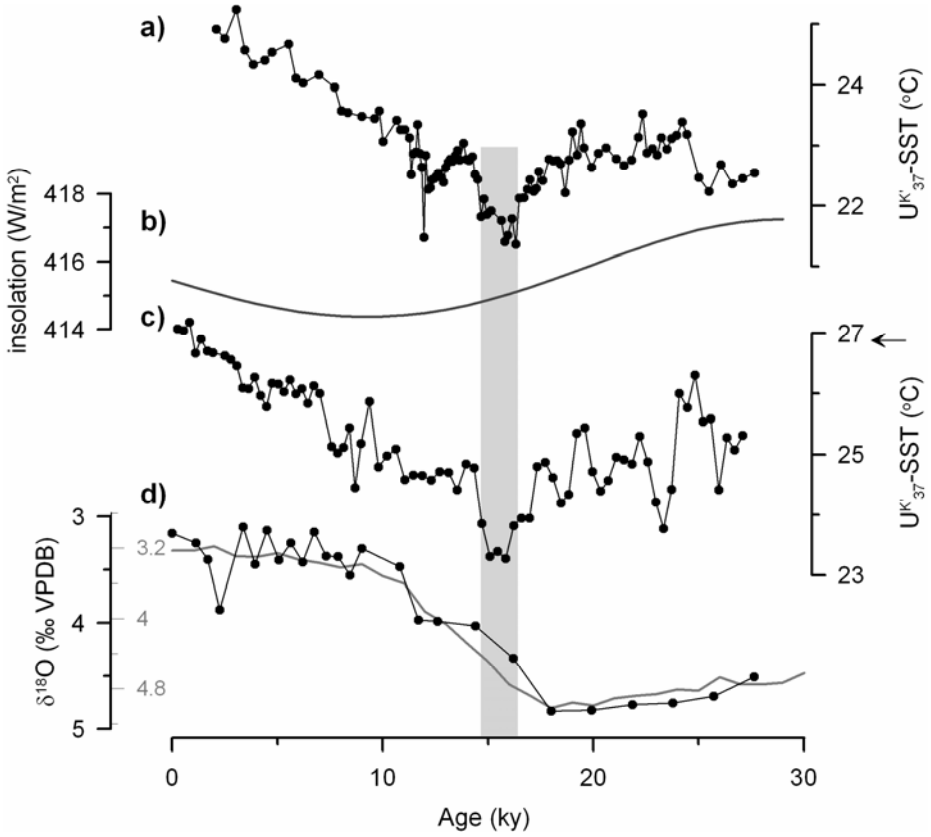


**Figure 6:** a) Alkenone-derived ($U_{37}^{K'}$) Sea surface temperature record from the eastern tropical Pacific (0°N) [*Kienast et al.*, 2006]. b) Mean annual insolation at 5°N. c) $U_{37}^{K'}$-SST record from Panama Basin core KNR176-JPC32 (5°N). d) Benthic foraminiferal (*Uvigerina*) $\delta^{18}O$ record and the global benthic $\delta^{18}O$ stack of *Lisiecki and Raymo* [2005]. Gray bar marks the early deglacial SST cooling that coincides with Heinrich event H1.

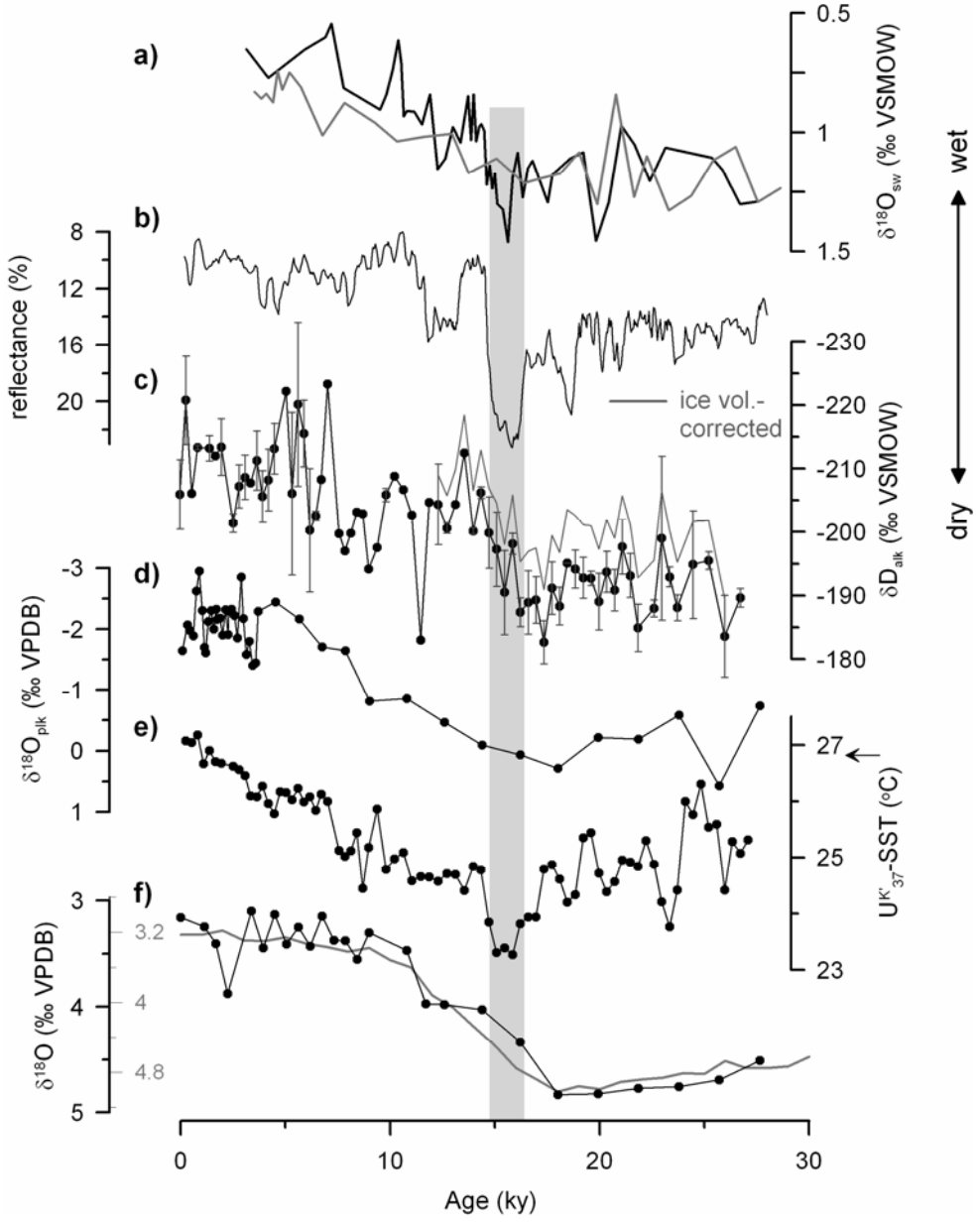


**Figure 7:** Paleo-records along core JPC32 compared to $\delta^{18}O_{sw}$ records from the Caribbean and the Cariaco Basin reflectance record. a) $\delta^{18}O_{sw}$ records from the Caribbean (ODP Site 999A (gray), VM28-122 (black) corrected for global ice volume changes using Waelbroeck *et al.* [2002]) that reflect changes in surface water salinity and thus precipitation [*Schmidt et al.*, 2004]. b) Reflectance record from the Cariaco Basin (ODP Site 1002) indicating changes in precipitation and runoff [*Peterson et al.*, 2000]. c) $\delta D_{alk}$ record along core JPC32 (black); gray curve is $\delta D_{alk}$ corrected for mean ocean δD changes (using the mean ocean $\delta^{18}O$ curve of *Waelbroeck et al.* [2002] converted to δD using $\delta D = \delta^{18}O*8.13+10.8$ [*Rozanski et al.*, 1993]) (Note inverted δD axis). d) *G. bulloides* $\delta^{18}O$ record from JPC32. e) $U_{37}^{K'}$-derived SST record, arrow marks mean annual atlas SST at the core site [*Levitus and Boyer*, 1994]. f) Benthic foraminiferal (*Uvigerina*) $\delta^{18}O$ record and the global benthic $\delta^{18}O$ stack of *Lisiecki and Raymo* [2005]. Gray bar marks the early deglacial $\delta D_{alk}$ decrease and associated SST cooling that coincide with Heinrich event H1

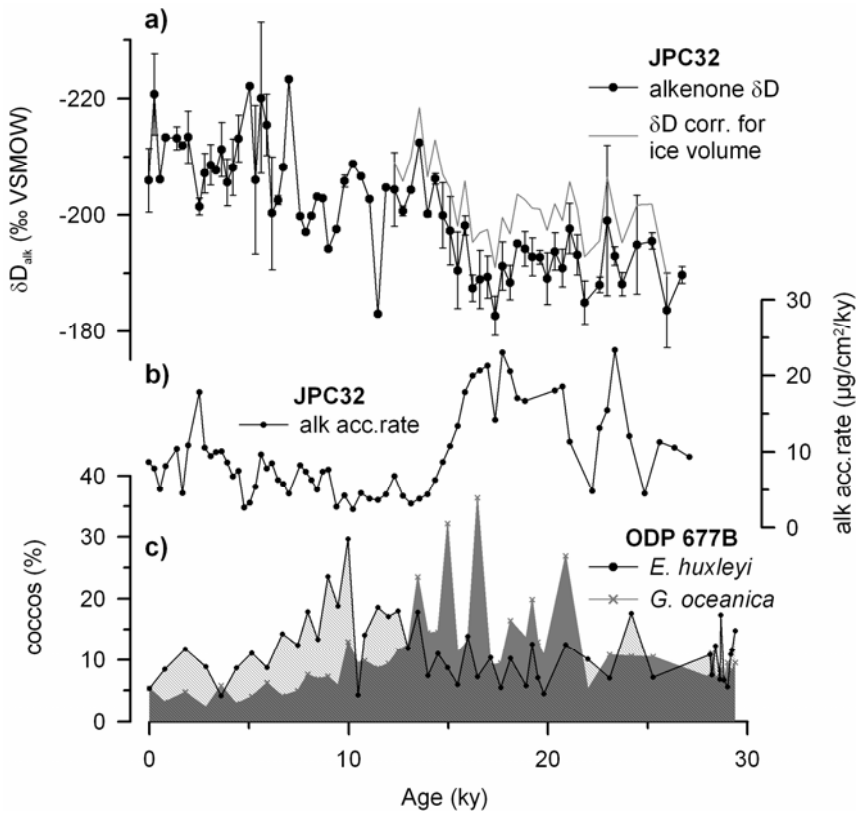


**Figure 8:** a) Alkenone δD record (note inverted δD axis) and b) alkenone accumulation rates along core JPC32 compared to c) coccolithophorid (*E. huxleyi* and *G. oceanica*) abundances in ODP core 677B [*Martínez et al.*, 2006].

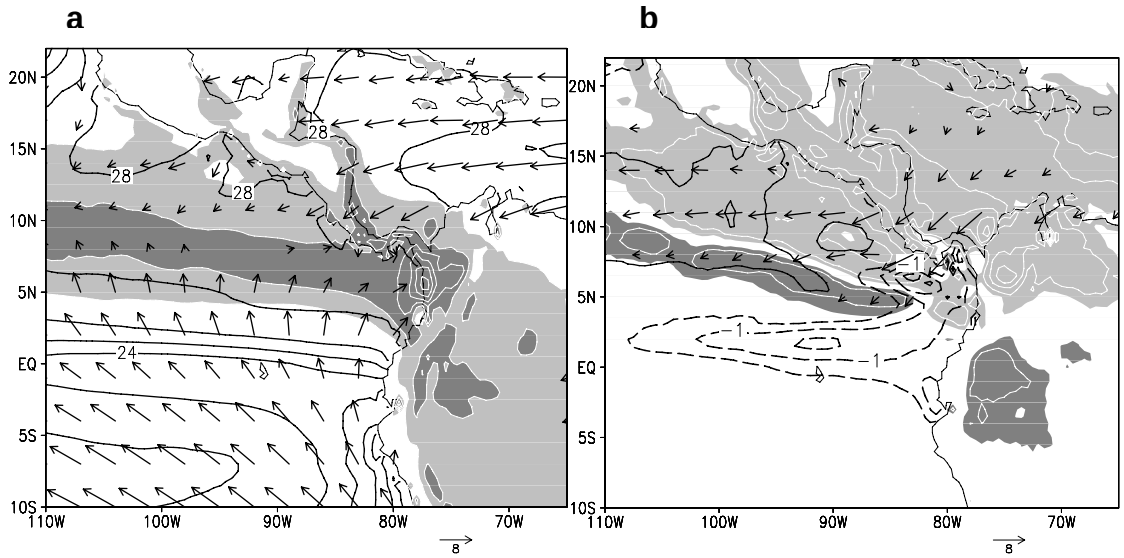


**Figure 9:** (a) Annual-mean climatology of SST (contours at intervals of 1$^{o}$C), precipitation (white contours at intervals of 5 mm/day; light and heavy shade > 5 and 10 mm/day), and surface wind velocity (m/s) in ROAM. (b) JAS anomalies in the "water-hosing" run: SST (black contours at 0.5$^{o}$C intervals, with the zero contour omitted and negative values dashed), precipitation (white contours at 5 mm/day intervals; dark shade > 2.5 mm/day, and light shade < -2.5 mm/day), and surface wind velocity (< 1.5 m/s omitted for clarity) (see appendix for more details).